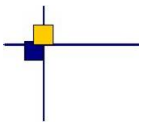

Mean Sea Level from Altimetry and Tide-Gauges

Annual Report 2021

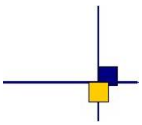

Reference : SALP-RP-MA-EA-23541-CLS

Nomenclature : 2021 Annual Report MSL/TG

Issue : 1.2

Date : March 17, 2022

CLS - 8-10 Rue Hermès - Parc Technologique du Canal - 31520 Ramonville St-Agne - FRANCE
Telephone 33 5 61 39 47 00 / Fax 33 5 61 75 10 14

Chronology Issues:		
Issue:	Date:	Reason for change:
1.0	January 6, 2022	Creation
1.1	February 24, 2022	Internal version
1.2	March 17, 2022	Public version

People involved in this issue :				
	AUTHORS	**COMPANY**	**DATE**	**INITIALS**
Written by:	A. Guérou	CLS	January 6, 2022	AG
Checked by:	P. Prandi	CLS	January 25, 2022	PP
Approved by:				
Application authorised by:				

Distribution:		
Company	Means of distribution	Names
CLS	electronic copy	pprandi@groupcls.com slabroue@groupcls.com jlegeais@groupcls.com
CNES	electronic copy	thierry.guinle@cnes.fr gerald.dibarboure@cnes.fr francois.bignalet-cazalet@cnes.fr nicolas.picot@cnes.fr benoit.meyssignac@cnes.fr

Applicable documents / reference documents

RD1 - Annual report MSL/TG 2016 - Prandi, Valladeau, and Debout [1]
RD2 - Annual report MSL/TG 2017 - Ablain, Taburet, Zawadzki, Jugier, and Vayre [2]
RD3 - Annual report MSL/TG 2020 - Guérou [3]
RD4 - Calval report Jason-3 GDR-F - Roinard and Coquelin [4]

Contents

List of tables and figures

List of Tables

List of Figures

List of Acronyms

AVISO Archiving Validation and Interpretation of Satellite Oceanographic data. 1–4, 21–23

CalVal Calibration and Validation. 6

CLS Collecte Localisation Satellites. 4, 20

CMEMS CMEMS. 4, 20

CNES Centre National d'Etudes Spatiales. 1, 4, 14, 15, 20

GC GLOSS-CLIVAR. 3, 4, 20, 21, 24–29

GDR Geophysical Data Record. 1, 6, 18

GIA Global Isostatic Adjustement. 3

GMSL Global Mean Sea Level. 1–5, 7, 9–19, 24, 25, 28

J 1 Jason-1. 2–4, 18, 19, 24, 25, 28

J 2 Jason-2. 2–4, 18, 19, 24, 25, 28

J 3 Jason-3. 2–4, 6–19, 24–26, 28

L2P 18 Level-2 + 2018. 3, 28

L2P 21 Level-2 + 2021. 1–4, 8, 18–20, 28

LRM Low Resolution Mode. 14

MSL Mean Sea Level. 1–5

NTC Non Time Citical. 14

OLS Ordinary Least Square. 7, 14

PLRM Pseudo Low Resolution Mode. 1, 3, 9–13, 26, 27

PSMSL PSMSL. 3, 4, 20, 21, 24–26, 28

PTR Point Target Response. 2, 9, 12

REFMAR REFMAR. 20

RMS Root Mean Square. 4, 18, 19

S3A Sentinel-3A. 2–4, 6–10, 12, 25–28

S3B Sentinel-3B. 1–3, 6, 10–13, 25, 27

S6A Sentinel-6A MF. 1–4, 6, 14–17

SALP Service d'Altimétrie et de Localisation Précise. 1, 4

SAR Synthetic Aperture Radar. 1, 3, 9–14, 26, 27

Saral Saral/AltiKa. 2–4, 6–8, 10, 11, 25, 26

SLA Sea Level Anomaly. 4, 14, 20, 21

TG Tide-Gauges. 1–4, 20–25, 27, 28

TP TopEx-POSEIDON. 1–4, 6, 18–20, 24, 25, 28

TP-A TopEx-A. 2, 4, 14, 18, 19

TP-B TopEx-B. 2, 4, 18, 19

USO Ultra Stable Oscillator. 2, 3, 10–12

VLM Vertical Land Motion. 3, 24, 25

WTC Wet Tropospheric Correction. 2–4, 6–8, 11, 12, 15, 16

1. INTRODUCTION

This document is the 2021 annual report of the Mean Sea Level activities conducted within the CNES/SALP framework. This report contains two main chapters:

2. **Analysis of the Mean Sea Level indicator measured by the altimetry**
3. **Analysis of the Mean Sea Level indicator measured by the Tide-Gauges networks**

Most of the activities presented here are the follow-on of the activities presented in the 2020 MSL SALP annual report [3]. The main achievement of the year 2021 is the dissemination of the new version of the GMSL climate indicator on the AVISO website, based on the L2P 21 data products. This new dataset will be associated to a peer-review publication (Guérou et al., 2022) that is currently under internal revision and that contains a detailed discussion on the limiting factors of the GMSL long-term stability. These results are not presented in the report since most of the results were presented in the 2020 annual report.

A long list of activities on the Sentinels missions were achieved this year, presented in Chapter 2.. The main achievements are: the full understanding of the Sentinel-3B GMSL drift, in both SAR and PLRM (see Section 2.2.3.), and the analysis of the commissioning data of the new reference mission Sentinel-6A MF (Section 2.2.4.), launch in October 2020. A new GDR product of the TopEx-POSEIDON mission is under production (F standards) and preliminary analysis of the associated GMSL timeseries is presented in Section 2.2.5.

Finally, we present the comparison of the altimetry based GMSL with Tide-Gauges data in Chapter 3. A focus is given on the detection and estimation of potential long-term drift of the altimetry missions thanks to the estimation of uncertainties.

2. Mean Sea Level indicator

2.1. Updates of the AVISO webpages

In 2021, the AVISO webpages on the Mean Sea Level have been updated: both the layout/content of the pages and the distributed MSL data, with the dissemination of the L2P 21 GMSL ocean indicator products (see the following News).

The main idea was first, to get clearer and simplify messages on the scientific topic, and second, to ease the data access on only one page that is well identified within the AVISO webpages. We invite the reader to navigate through the website to see all the updates.

In the following subsections, we summarise the main results on the new L2P 21 GMSL climate indicator that is disseminated on AVISO.

2.1.1. The reference missions

The GMSL climate indicator obtained from the reference missions TP, J 1, J 2, J 3 based on the L2P 21 products is shown in Figure 1. The only major update of the climate indicator as compared to the 2020 annual report analysis (see Section 2.2 of RD3) is the update of the associated uncertainty budget (in particular the intermissions offset and the J 3 radiometer uncertainties). The construction of this new uncertainty budget will be available in Guérou et al. (2022, in prep).

We recall that, to this date, the GMSL timeseries available to download on AVISO is not corrected for the suspected drift of the TP mission (Valladeau et al. [7], Watson et al. [8], Dieng et al. [9], Beckley et al. [10], Cazenave et al. [11], Legeais et al. [12]). Only an illustration of this corrected timeseries (as in Figure 1) is given on the AVISO main page. We note that such correction (from Ablain et al. [5]) has been added to the Copernicus C3S dataset following the decision reported in the 2020 annual report [RD3].

For information, in Figure 2, we provide the sea level estimates of the L2P 21 GMSL after correction of the TP drift. Significant acceleration of $0.12 \pm 0.06\ mm.yr^{-2}$ is thus detected whereas it is not when one does not consider the TP drift correction. The first order coefficient is also reduced from $3.5\ mm.yr^{-1}$ to $3.3\ mm.yr^{-1}$.

2.1.2. Cross comparison between altimetry missions

The evolution of the GMSL time series for most of the altimetry missions (past and in-flight) is plotted in Figure 3. The data shown here is based on the L2P 21 products. The different reference missions have been inter-calibrated in term of GMSL biases using their tandem-phases whereas the GMSL time series of the so-called "opportunity" missions (all others than TP, J 1, J 2, J 3) are inter-calibrated using the L2 least square norm with respect to the reference GMSL time series. Such a normalisation is applied once for each "opportunity" missions over the first common period with a reference mission (i. e. , Saral/AltiKa with J 2 only). This differs from the method used previously (see Section 2.2.2. in RD3) where a new intermission offset was derived if the opportunity satellite's orbit changed and/or the reference mission changed.

The Sentinels missions S3A and S3B are not plotted in this figure, neither distributed on the AVISO website, since they are subject to significant drift anomalies (see the respective Sections 2.2.2. and 2.2.3.). When

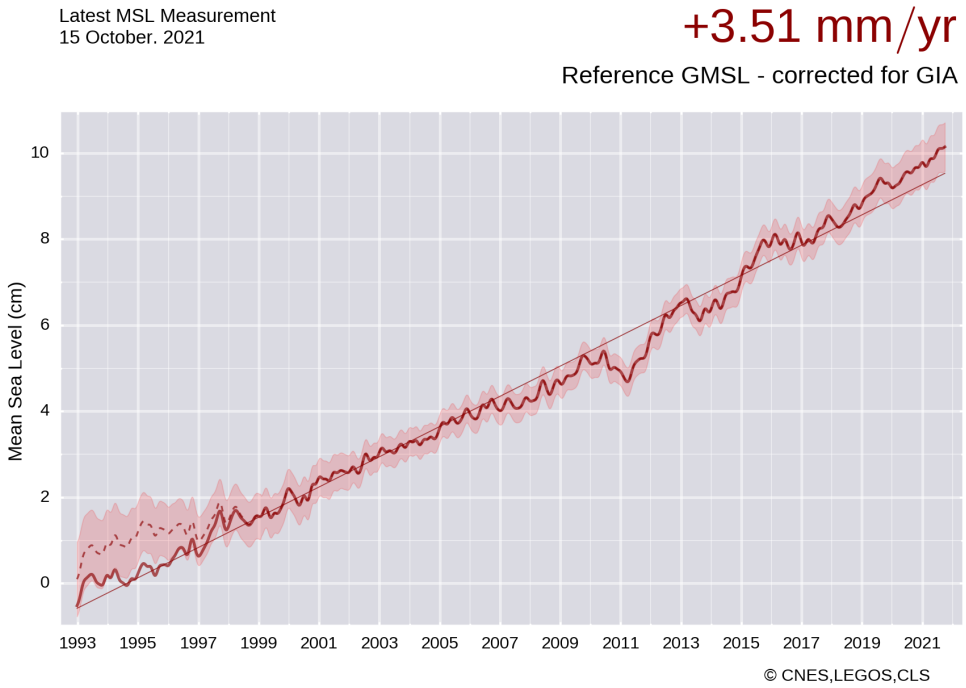

Figure 1: Global Mean Sea Level indicator as observed by the reference missions: TP, J1, J2, J3, using the L2P21 geophysical standards. The red envelop corresponds to the 90% confidence level uncertainties. The seasonal signals have been removed, a 6-months filter has been applied as well as a correction $+0,3mm/yr$ corresponding to the GIA. The dashed line corresponds to the TP drift correction from Ablain et al. [5].

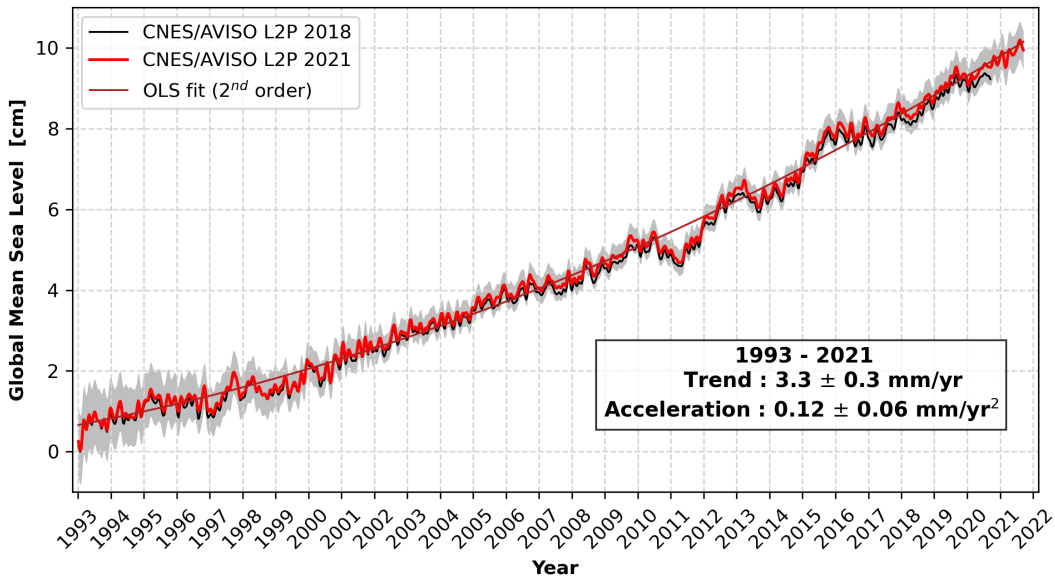

Figure 2: Global Mean Sea Level indicator as in Figure 1, corrected from the TP drift correction from Ablain et al. [5]. A significant acceleration is thus observed. The timeseries is filtered with a 2-months Lanczos fitler. The L2P18 version is shown for comparison. Figure from Guérou et al. (2022, in prep).

such anomalies will be solved, we will consider including them on the AVISO GMSL pages.

The interest of such comparisons is to highlight the relative good homogeneity of all the missions in terms of GMSL evolution, as well as to highlight discrepancies (reaching 1 cm for some missions, e. g. , Envisat in 2003, ERS-1 in 1999) and the relative good agreement between all missions in the recent years. We note that solutions between Jason-3 and Saral/AltiKa are diverging from 2016-2017 to present days. Multiple reasons could explain this: a potential radiometer WTC drift of J 3 (under investigation, see Section 2.2.1.1.) and/or the aging of the Saral altimetry mission (see Section 3.2.2.). We do not investigate further this topic in this report but will do in 2022.

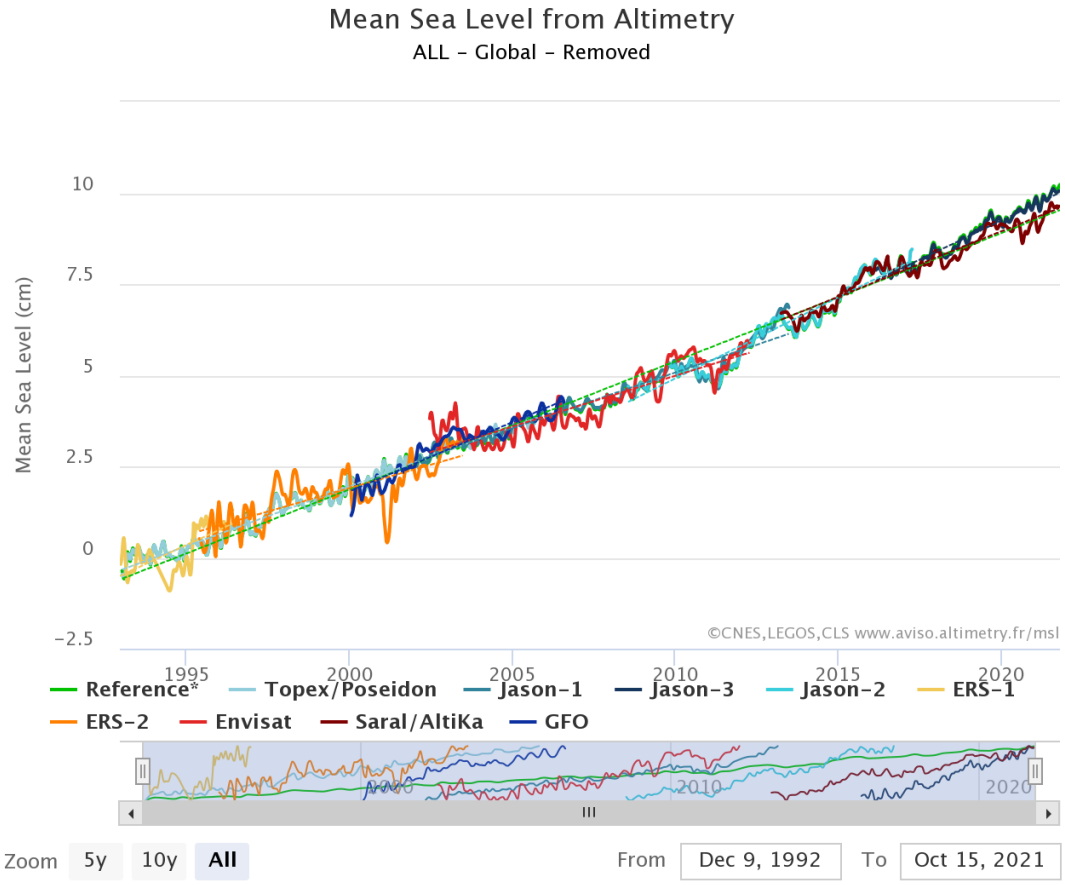

Figure 3: GMSL indicator as observed from all altimetry missions with the use of the L2P 21 geophysical standards. Illustration taken from AVISO.

2.1.3. Mean Sea Level at the regional scale

The spatial distribution of the regional MSL trends is derived from the multi-mission L4 gridded sea level products (1/4 deg.) distributed by the Copernicus Services (data directly available here). We use the two-satellites version from the C3S service that is well suited (and recommended) for climate study (see dicussion in Section 2.3. of RD3). The related documentation is available on the C3S product page and the associated processing is detailed in Taburet et al. [13]. This indicator map is produced by CLS in the context of the CNES/SALP project and distributed on the AVISO MSL webpage, as well as on the CMEMS webpage.

The current version of the regional MSL trend map (Figure 4) currently covers the period January-1993 to

December-2020 and will be extended to June-2020 during the first 2022 semester. We note that the regional MSL variations are larger than the GMSL ones due to the large local variability generated by regional changes in winds, pressure, and ocean currents which average out at global scale [14]. The regional MSL trends exhibit large scale variations with amplitudes ranging from -3 to $8\,mm/yr$ in regions such as the western tropical Pacific Ocean, the boundary current systems and the Southern Ocean. A part of these regional variations is related to the inter-annual variability of the ocean (e. g. , ENSO events).

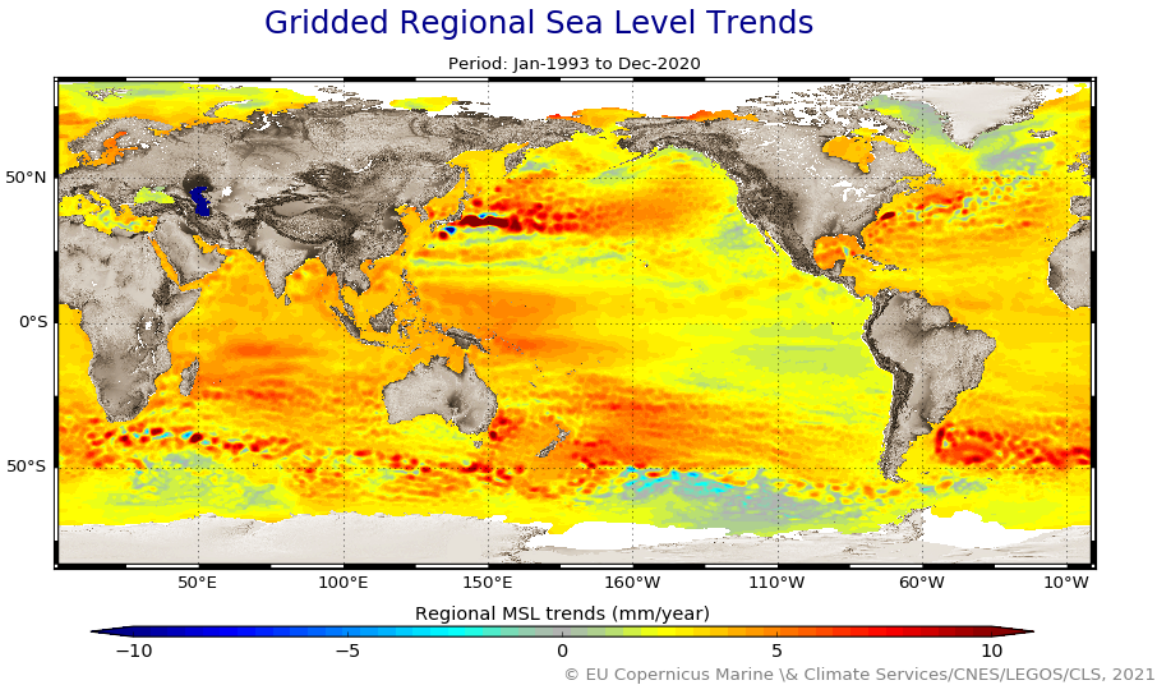

Figure 4: Regional MSL trends from the multi-missions L4 CMEMS gridded products over the period September-1992 to June-2020

2.2. CalVal activities

This section summarises the various Calibration and Validation activites focused on the climate research and the long-term stability of the altimetry data records. Specific sections are dedicated to the the following missions:

- Jason-3, Sect. 2.2.1.
- Sentinel-3A, Sect. 2.2.2.
- Sentinel-3B, Sect. 2.2.3.
- Sentinel-6A MF, Sect. 2.2.4.
- TopEx-POSEIDON, Sect. 2.2.5.

2.2.1. Jason - 3

New GDR-F standards have been released in 2021 for Jason-3 (see Calval report RD4). This year, we have performed new investigations on the long-term stability and quality of this dataset, in particular:

- The stability of the radiometer WTC, Section 2.2.1.1.
- The impact of the adaptive retracking onto the stability of the record, Section 2.2.1.2..

2.2.1.1. Jason-3 WTC drift

As presented in the 2020 annual report (RD3), investigations have been performed to contribute to Barnoud et al. [6], now published, to estimate the contribution of J3 data to the non-closure budget of the sea level. We found that J3 altimeter is stable within an uncertainty of $0.4\ mm/yr^{-1}$ (90 % C.L.) but some suspicion had been raised about the stability of its radiometer data. Indeed, based on Figure 5 (from Barnoud et al. [6]), a systematic drift of the radiometer data has been found as compare to Saral ($0.8\ mm.yr^{-1}$) and S3A ($0.5\ mm.yr^{-1}$) radiometer data.

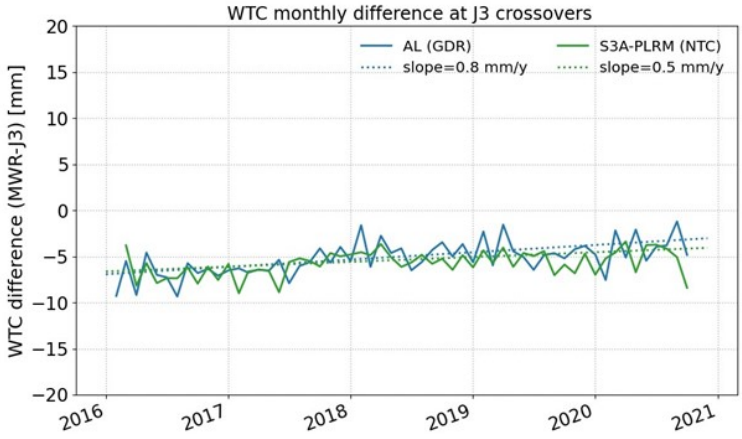

Figure 5: Monthly crossovers differences of the WTC radiometer data between Jason-3, Sentinel-3A and Saral/AltiKa. From Barnoud et al. [6, supplementary material].

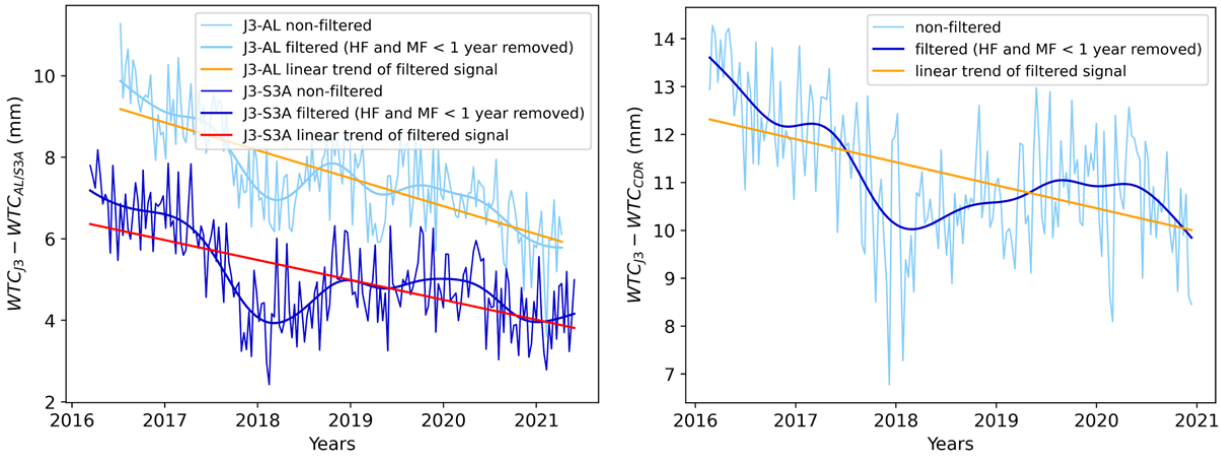

Figure 6: Comparison of WTC GMSL-like timeseries from Jason-3, Sentinel-3A and Saral/AltiKa radiometers (left panel) and from Jason-3 radiometer and WTC solution from the SSMI-based CDR of water vapor. Courtesy of Magellium for the figure.

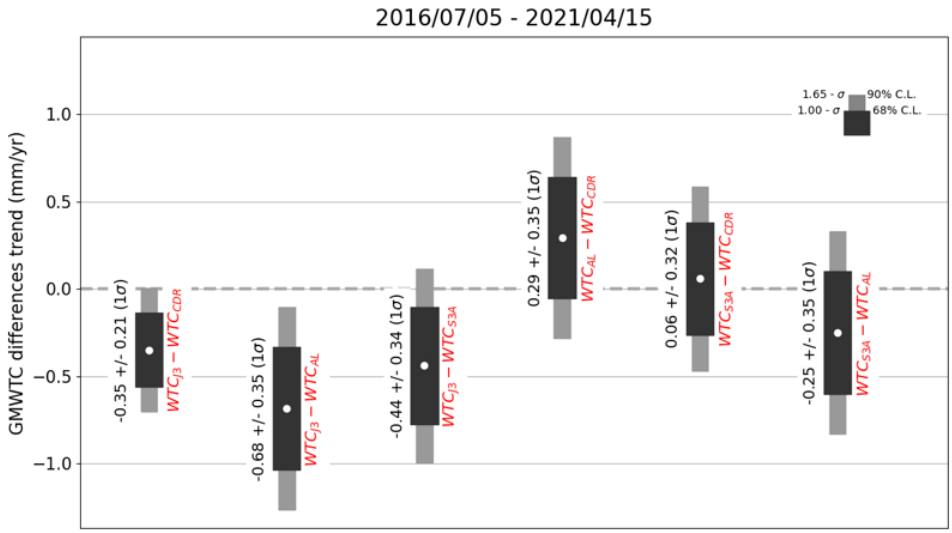

Figure 7: Summary of the drift and associated uncertainties measured between the WTC solutions from the Jason-3, Sentinel-3A and Saral/AltiKa radiometers, and the SSMI-based CDR of water vapor content. Courtesy of Magellium for the figure.

In 2021, further investigations have been performed within the SALP framework, in collaboration with Magellium, to better quantify the suspected drift. We performed direct comparisons of the WTC solutions from Jason-3, Sentinel-3A and Saral/AltiKa radiometers. In other words, we computed a GMSL-like WTC for each radiometer, i. e. , a weighted global average of the the along-track data, and make the differences between them. The respective timeseries are shown in Figure 6 (left panel). In addition, thanks to an uncertainty budget approach and an OLS estimator, we estimated the relative drift along with their uncertainties to accurately quantify the potential GMSL drift induced by the radiometers data (summarised in Figure 7). A full description of this approach is given in Jugier et al. [15, submitted].

Similar comparison of the J3 radiometer data has also been made with a WTC computed from a water vapour Climate Data Record (CDR) based on the SSMIs radiometer data (Figure 6, right panel). Such

CDR is considered as very stable due to the very accurate calibration of the SSMI intrument. An in-depth description and analysis of such CDR is presented in Barnoud et al.(2022, submitted). From such analysis, similar drift is found between CDR and J3 WTC timeseries as between J3 and Saral and/or S3A data, i.e., $-0.4 \pm 0.3\ mm.yr^{-1}$. It is important to notice that the L2P21 data v3.0 were used for all three altimetry missions, J3 data thus containing both GDR-D and GDR-F data.

Based on these analyses, we found that J3 WTC radiometer data is drifting by $\sim 0.6 \pm 0.3\ mm.yr^{-1}$ over the period 2016-2021. This latter value is the one used to update the uncertainty budget in Guérou et al. (2022, in prep.)

2.2.1.2. Adaptive retracking on Jason-3 GDR-F

Part of the new GDR-F standards of the J3 data, a solution based on the adaptive retracking is distributed. The performance analysis has already been addressed in the 2020 annual report RD3 but was covering the 2016-2019 period only. Here we present similar results to the 2020 annual report considering the entire GDR record available, from March 2016 to December 2020.

Extract from Roinard et al. (2022, in prep.) about the Jason-3 GDR-F L2 data quality assessment:

"*Jason-3 altimetry mission is the current reference mission that monitor the GMSL climate indicator. Such indicator is derived from the along-track L2 data by performing a weighted mean per regional areas over each mission's cycle. The details of the computation can be found in the aviso website. We analyze the different GMSL solutions based on the Jason-3 data: [...] GDR-F with MLE-4 retracking and with adaptive retracking. [..] We also compared the different retracking solutions provided in the GDR-F data by computing the GMSL difference between the adaptive and the MLE4 solutions (Figure 8). A very good consistency is observed (differences are submillimeter) but a jump (about 6mm) is observed from September-2017 and June-2018. This corresponds to instrument resets (upload of the DEM at cycle 057 and BDR update at cycle 085), and differences in the echo centering between these cycles. These differences in the echo centering are visible in the difference between the two retracking solutions since the adaptive solution takes them naturally into account, whereas the MLE4 calibrations (LUT) are only based on the instrument characteristics at the beginning of the mission. It also can indicate that potential changes in the PTR have occurred and that these changes may not have been accounted for in the internal path delay. We recall that the LUT (only applied during MLE4 processing) have been computed only once at the beginning of the mission and never updated since then. As shown by the two panels of Figure 8, the adaptive solution does not impact the slope of the Jason-3 GMSL over the 5 years of the mission, as compared to the GDR-F MLE-4 solution. This is the case both when considering (left panel) or ignoring (right panel) the time interval where the jump is observed. As a conclusion, the adaptive solution conserves the stability of the GMSL record and allows to naturally prevent anomalies in the instrument calibrations over the lifetime of the mission.*"

An interesting investigation to be performed in 2022 will be the estimation of the reduction/increase of the correlated noise at 2-months and 1-year (that is used in the uncertainty budget) between the MLE4 and adaptive retracking solutions. From Figure 8 and the jump observed, this could potentially be an additional argument to choose the adaptive retracking for climate studies.

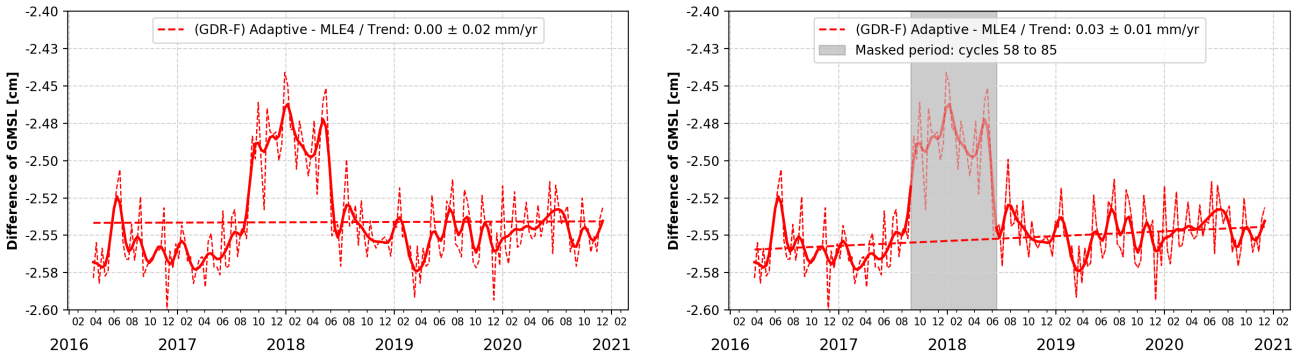

Figure 8: J3 GMSL difference between GDR-F adaptive and MLE4 with (left) and without removal of cycles 057 to 085 (right).

2.2.2. Sentinel-3 A

Sentinel-3A has been launched in 2016 and was the first altimetry mission to operate in both SAR and PLRM modes. Significant long-term drift of its SAR mode has been detected in 2019 and many investigations have been performed part of the MPC S3 consortium. As of today, the Sentinel-3A SAR drift has been understood and attributed to, mainly, some approximations in the processing of lateral look range. Such approximations can now be corrected by applying the so called "range walk correction". In a second order, significant PTR evolution of the on-board altimeter also caused long-term drift of about 0.2 -$0.3\ mm.yr^{-1}$ due to approximations in the ground segment processing (see Section 2.4.1.2 of the 2020 annual report [RD3] for more details).

In 2021, preliminary tests have been performed on the ground-segment processing and in particular on the implementation of the range walk processing. Figure 9 shows some results presented by S. Dinardo at the 8^{th} Sentinel-3 ESL council meeting. The curve shows the difference of S3A SAR solutions with and without range walk applied on the Level-1 data. The test has been performed on a regional area over the pacific ocean and the resulting Level-2 data have been simply daily averaged.

From Figure 9, one observes drifts of $-2.1\ mm.yr^{-1}$ over the year 2016 and of $-0.3\ mm.yr^{-1}$ over the period 2017-2021. These figures are similar to the one observed between the SAR and PLRM GMSL time-series, over the same periods, as shown in Figure 10. We recall that the PLRM mode is not affected by the azimuth Doppler effect as the SAR mode and thus does not drift over time due to this process (still others drift cause could exist). As a consequence, we demonstrate with this dataset that the range walk explains well the discrepancies observed between SAR and PLRM modes over long periods.

It is important to keep in mind that other effects such as PTR evolution can also translate as long-term drift, but affects SAR and PLRM mode in very similar manner. Such effect is not corrected by the range walk processing but thanks to adapted numerical retracking such as the "adaptive" retracking (see Section 2.2.1.2.).

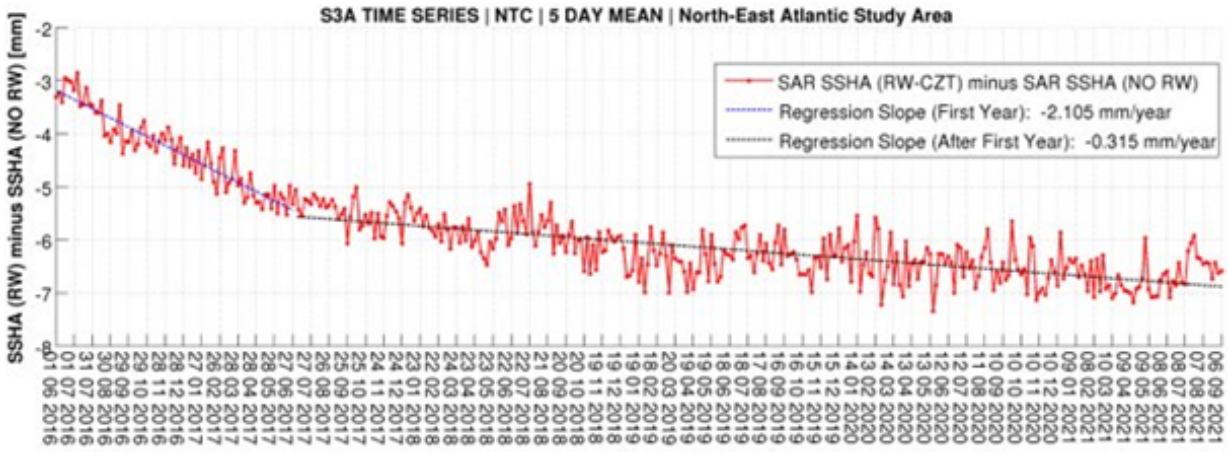

Figure 9: Daily mean SSHA differences of Sentinel-3A SAR data with and without "range walk" processing applied. The dataset is limited to a regional area over pacific.

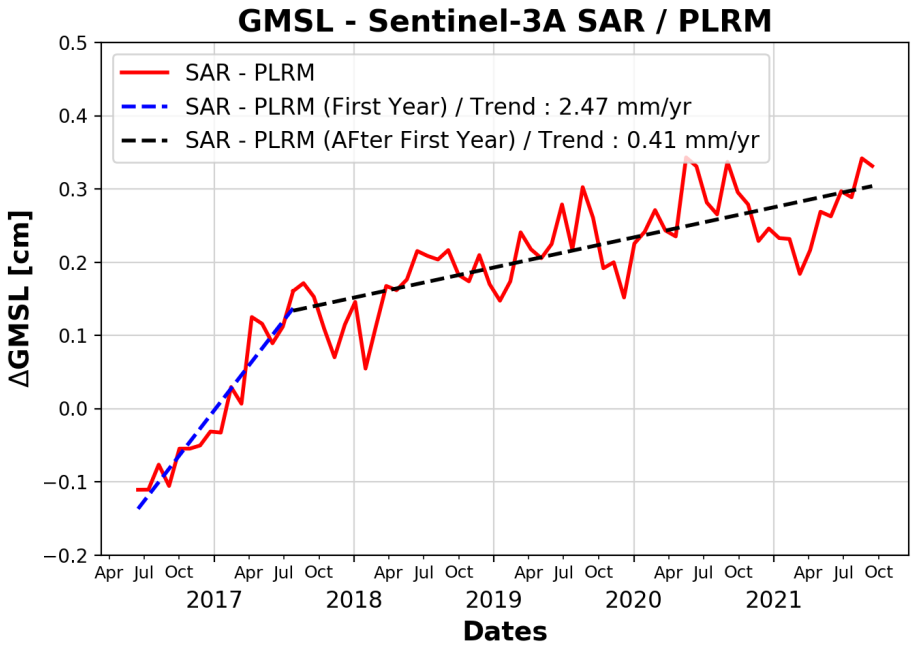

Figure 10: GMSL differences of Sentinel-3A SAR and PLRM official PDGS data.

2.2.3. Sentinel-3 B

The Sentinel-3B altimetry mission has been launched in 2018 and is part of the Copernicus program. Since its launch, its derived GMSL timeseries has been showing no sea level rise, both in SAR and PLRM modes.

Recent investigations presented by S.Dinardo at the 8^{th} Sentinel-3 ESL council meeting showed an anomaly in the use of the Ultra Stable Oscillator (USO) parameters in the official ground segment. By correcting this anomaly, it has been showed that the S3B GMSL timseries is in agreement, within uncertainties, with the other altimetry missions currently in orbit, i. e. , Jason-3, Saral/AltiKa and Sentinel-3A.

In the following paragraph, we first show the impact and resolution of the USO anomaly (Sect 2.2.3.1.) and then highlight that a small drift discrepancies remains between the SAR and PLRM modes of S3B (Sect 2.2.3.2.) due to the lack of range walk processing of the SAR data.

2.2.3.1. Sentinel-3B Ultra Stable Oscillator

We derived the GMSL climate indicator for S3B PDAP data (with and without USO correction), over the period December 2018 – September 2021, and with J3 GDR-F data over the same period. We used the WTC from the radiometers for both missions despite the larger uncertainties associated to the one of J3 (see Sect 2.2.1.1.). For such short period (3 years), the uncertainties associated to the 2-months and 1-year correlated errors considered in the error budget are dominating, i.e., potential radiometer drift will not strongly affect our results. However, for an in depth analysis, similar comparison should be performed with WTC solutions from models. We show the results in Figure 11.

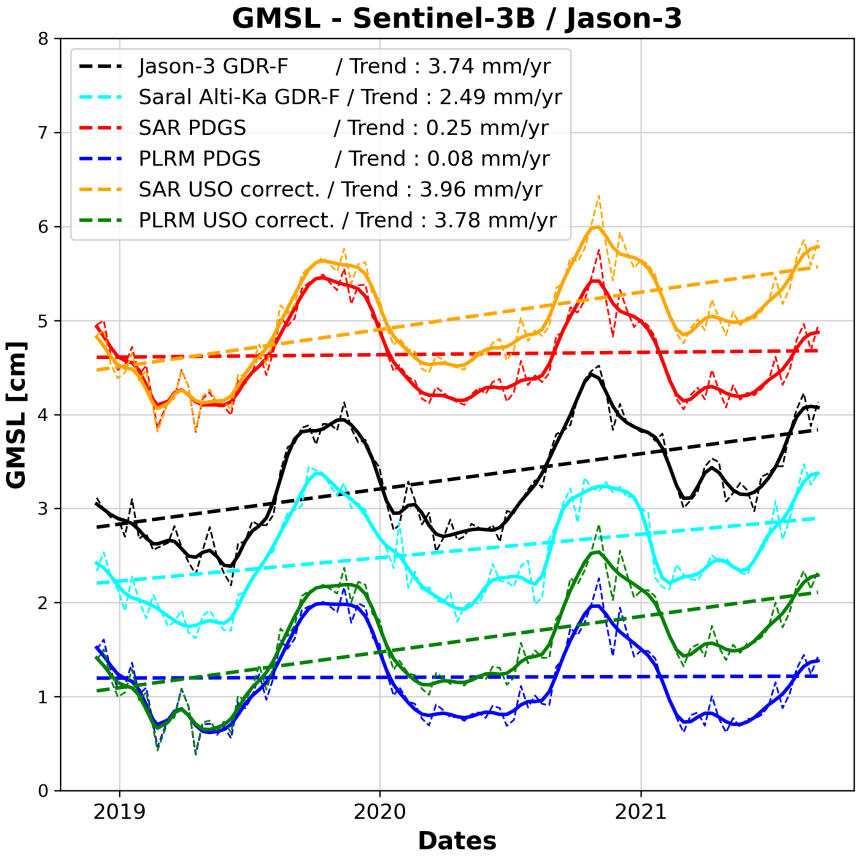

Figure 11: GMSL timseries of S3B (SAR and PLRM), with and without USO corrections, along with J3 and Saral. Respective trends are shown in the legend.

From Figure 11, we see that that the S3B GMSL trend has been corrected by $\sim 3.7\ mm.yr^{-1}$ for both SAR and PLRM data when considering the correct USO parameters in the data processing. We thus obtain a GMSL trend of ~ 3.7 - $3.9\ mm.yr^{-1}$ for S3B, similar to the trends observed for J3 over the same period.

We performed a complete analysis of the GMSL trend differences and their respective uncertainties between S3B (SAR and PLRM) and J3 following the method presented in Jugier et al. 15, submitted. This latter method allows to estimate trend uncertainties thanks to an error budget approach as developped in Ablain

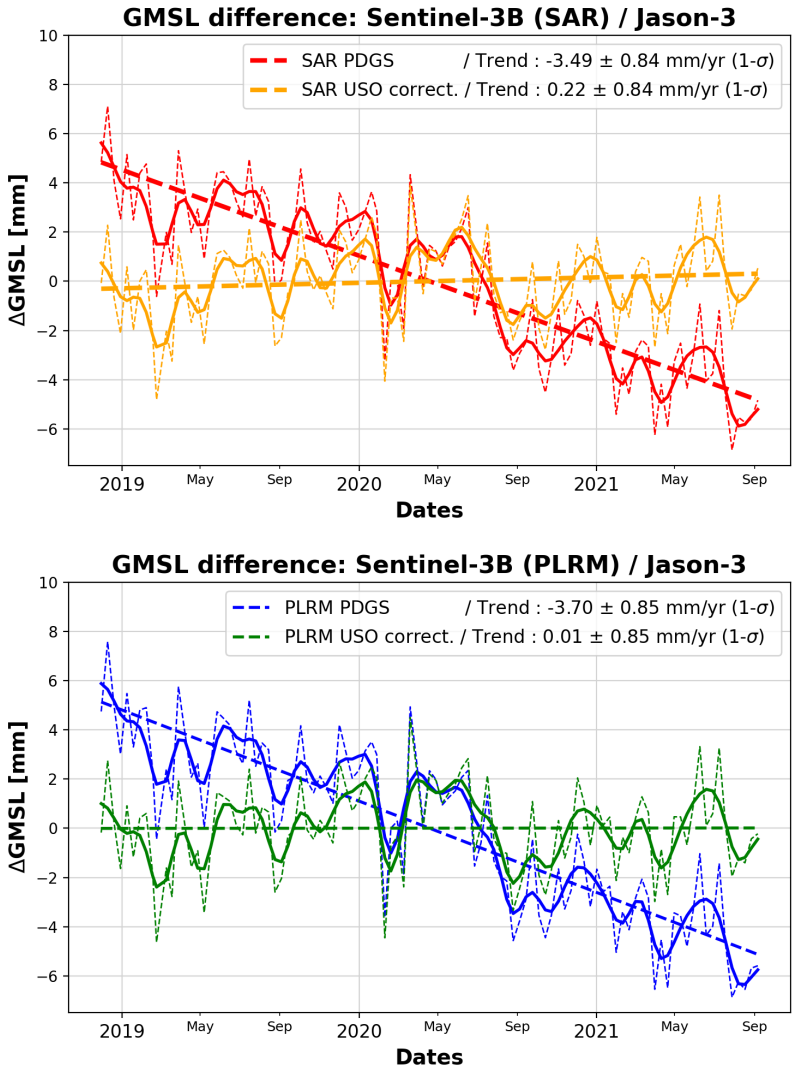

Figure 12: Relative GMSL drift estimations and their uncertainties between J 3 and S3B in SAR mode (top panel) and in PLRM (bottom panel). The WTC comes from the respective on-board radiometers

et al. [16]. Both GMSL timeseries are computed with the WTC from the respective radiometers. Our error budget considers the "high frequency noise" that we directly measured on the GMSL timeseries as well as the WTC correlated errors. The results are shown in Figure 12 for the SAR (top panel) and PLRM modes (bottom panel).

Thanks to the uncertainty estimations, we observe that thanks to the USO correction, S3B and J 3 GMSL now agree within the uncertainty of $0.9\ mm.yr^{-1}$ (1-σ). This high level of uncertainty is typical for such short period (3 years) but nevertheless allows to observe the improvement of the S3B long-term stability.

2.2.3.2. Sentinel-3B PTR

As for S3A, the range walk processing of the S3B SAR data is not applied in the official PDGS ground segment. Since the PTR parameter evolution of S3B is relatively strong, it creates a long-term drift discrepancies of the SAR data only (the PLRM is not affected).

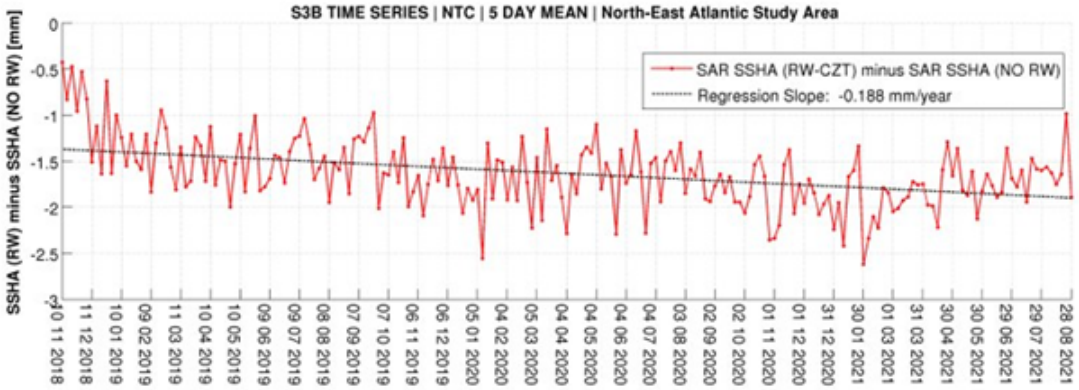

Figure 13: Daily mean SSHA differences of Sentinel-3B SAR data with and without "range walk" processing applied. The dataset is limited to a regional area over pacific.

In 2021, preliminary tests have been performed on the ground-segment processing and in particular on the implementation of the range walk processing. Figure 13 shows some results presented by S. Dinardo at the 8^{th} Sentinel-3 ESL council meeting. The curve shows the difference of S3B SAR solutions with and without range walk applied on the Level-1 data. The test has been performed on a regional area over the pacific ocean and the resulting Level-2 data have been simply daily averaged.

From Figure 13, one observes a drift of $-0.2\ mm.yr^{-1}$ over the 2019-2021. This figure is similar to the one observed between the SAR and PLRM GMSL timseries, over the same period, as shown in Figure 14. We recall that the PLRM mode is not affected by the azimuth Doppler effect as the SAR mode and thus does not drift over time due to this process (still, others drift causes could exist). As a consequence, we demonstrate with this dataset that the range walk explains well the discrepancies observed between SAR and PLRM modes over long periods. Furthermore, such correction would help to perfectly align S3B SAR mode to J3 GMSL record (see Figure 12).

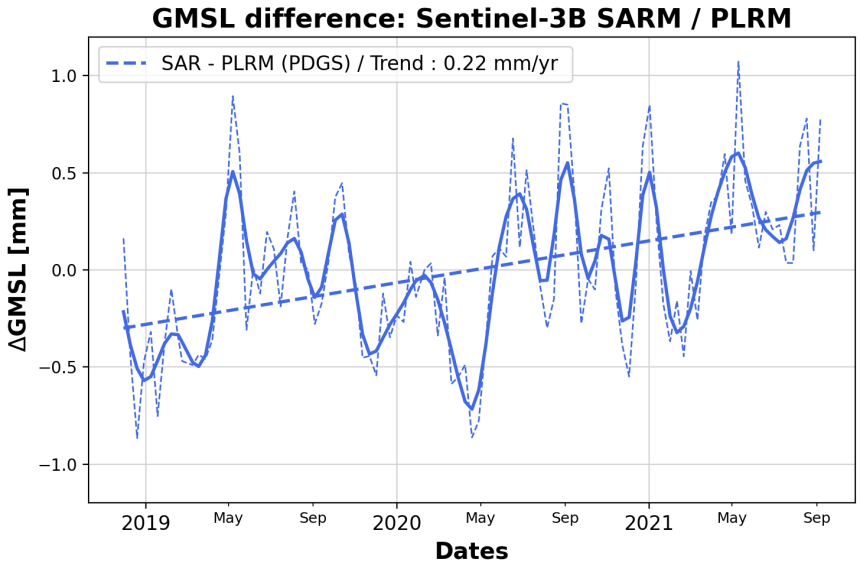

Figure 14: GMSL differences of Sentinel-3B SAR and PLRM official PDGS data.

2.2.4. Sentinel-6 A MF

The Sentinel-6A MF (S6A) altimetry mission has been launched in November-2020 and is in tandem phase with Jason-3 since then. It will become the reference mission during this year 2022. In the following sections, we summarise the various activities performed on the long-term stability assessment of the S6A GMSL data record as well as the quantification of its intermission offset uncertainty with Jason-3.

2.2.4.1. Sentinel-6A MF data status

We analysed NTC LRM data only, from two sources of data:

- **Official PDAP data from EUMETSAT**
  We used the data available as in December 2021 that contains data v 3.1 to v 3.3.2 (see documentation). This dataset contains a major update of the ionosphere correction in March 2021 which explains the jump observed at this date as well as the missing data for one cycle (cycle 13). A major anomaly has been detected on this dataset (AR 2168) that affect the long-term stability of the NTC data (see section 2.2.4.2.).
- **S6PP data from CNES ground segment prototype**
  This dataset benefits from the range walk processing for the SAR data and from a numerical retracking for both SAR and LRM data (see Dinardo et al., #3 S6VT 2021). These two latter processing are major improvements as compare as the official PDAP ground segment processing. We also note that the S6PP datasets uses the ionosphere correction from J 3 to derive the SLA variable of S6A.

These two datasets contains data from the side - A and side - B altimeters, with a switch occurring on the 14^{th} of September 2021. We recall that the switch of instrument has been pushed to guarantee high-quality intermission continuity in the case of the loss of the side - A altimeter during the mission lifetime. With the calibration of the side - B during the tandem phase, we ensure a low-level intermission offset uncertainty and thus a high-quality long-term stability of the GMSL record. Scenarios like the loss of the TP-A altimeter are thus avoided.

In Figure 15, we present the Sentinel-6A MF GMSL computed with these two respective datasets (NTC LRM data) along with the J 3 GMSL (top and middle panels). The comparison against J 3 shows that S6PP GMSL is stable as compared to J 3 with maximum differences of $\sim$ 4 mm, whereas PDAP NTC data shows trend differences and higher differences amplitude, i. e. , more than 10 mm (result of the open anomaly AR 2168). More detailed analyses of the timeseries are presented in the following Section 2.2.4.2. and Section 2.2.4.3..

2.2.4.2. Sentinel-6A MF drift anomaly

The anomaly AR 2158 (mentioned in the previous Section 2.2.4.1.) creates a drift of the Level-2 NTC range parameter. As part of the S6A commissioning activities, we investigated the exact impact of such anomaly onto the GMSL timeseries and verified that the S6PP datasets was not affected by any drifts originating from any other sources.

For each datasets, we computed the respective GMSL differences with J 3 and estimated the trend of the resulting timeseries along with their uncertainties thanks to an uncertainty budget approach based on an OLS estimator (as in Section 2.2.1.1.). A full description of this approach is given in Jugier et al. 15, (submitted).

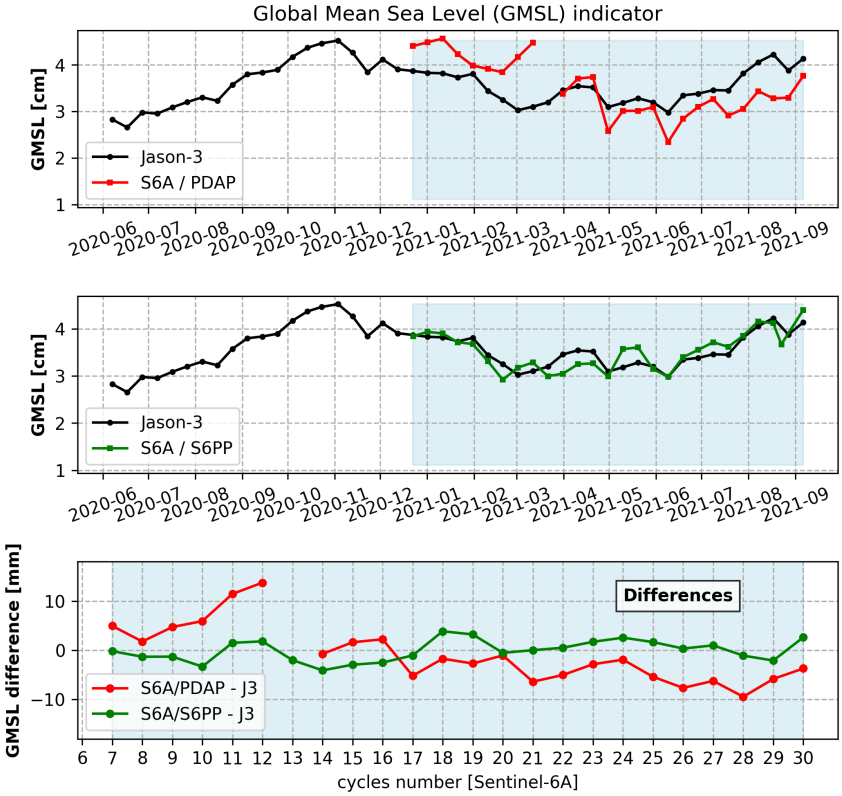

Figure 15: Sentinel-6A MF GMSL timseries over the tandem phase with Jason-3, for two datatsets: official PDAP data (top panel) and CNES S6PP prototype (middle panel). The discrepancies between the two missions are shown (bottom panel).

The uncertainty budget are adapted to the tandem phase configuration by considering only the non-correlated uncertainty sources between each altimetry missions, i. e. , non-correlated errors at 2-months ; and the WTC radiometer uncertainties. The former source of uncertainty is directly measured empirically onto the time-series whereas we use the value from Section 2.2.1.1. for the latter. Correlated errors at 1-year were not considered based on the analysis of the contribution of the sources of uncertainties presented in the 2020 annual report (RD3 - Section 2.2.4, i. e. , not strongly contributing as compare to the 2-months correlated errors at 8-months timescales). Finally, we remind the reader that the S6PP data contains Jason-3 ionosphere correction whereas PDAP data contains the true Sentinel-6A MF ionosphere correction. This might degrade the stability performance of the S6PP datasets. The respective uncertainty budget are presented in Table 1.

In Figure 16, we show the GMSL differences between J3 (GDRF) and S6A for PDAP NTC 1Hz data (top panel) and S6PP 1Hz data (bottom panel). We estimated the respective trends over the full period for the S6PP, and from cycle 14 inwards only for PDAP, as the data before this date contains many issues/jumps, etc. We find a trend of $-16 \pm 10\ mm.yr^{-1}$ (at 90% C.L.) between PDAP and J3 whereas the trend is estimated to $2 \pm 5\ mm.yr^{-1}$ (at 90% C.L.) for S6PP. Within the large uncertainties (expected on these short periods), one can say that PDAP data is drifting as compare to J3 whereas S6PP is not (within the uncertainties).

This result confirms the expected impact of the PDAP anomaly and shows that the S6PP processing allows to produce a S6A GMSL timeseries that is rather in-line with J3 GMSL.

Source of uncertainties	**Type of errors**	**Uncertainty (1-σ)**	**Method / References**
Altimeter noise / geophysical corrections	Correlated errors λ =2-months	$u_\sigma = 1.85\ mm$ for PDAP $u_\sigma = 1.3\ mm$ for S6PP	Empirically estimated
Radiometer WTC	Correlated errors λ =5-years	$u_\sigma = 1.6\ mm \Leftrightarrow 0.6\ mm.yr^{-1}$ over 5-years	Section 2.2.1.1.

Table 1: GMSL uncertainty budgets used to estimate the uncertainty drift between Sentinel-6A MF and Jason-3

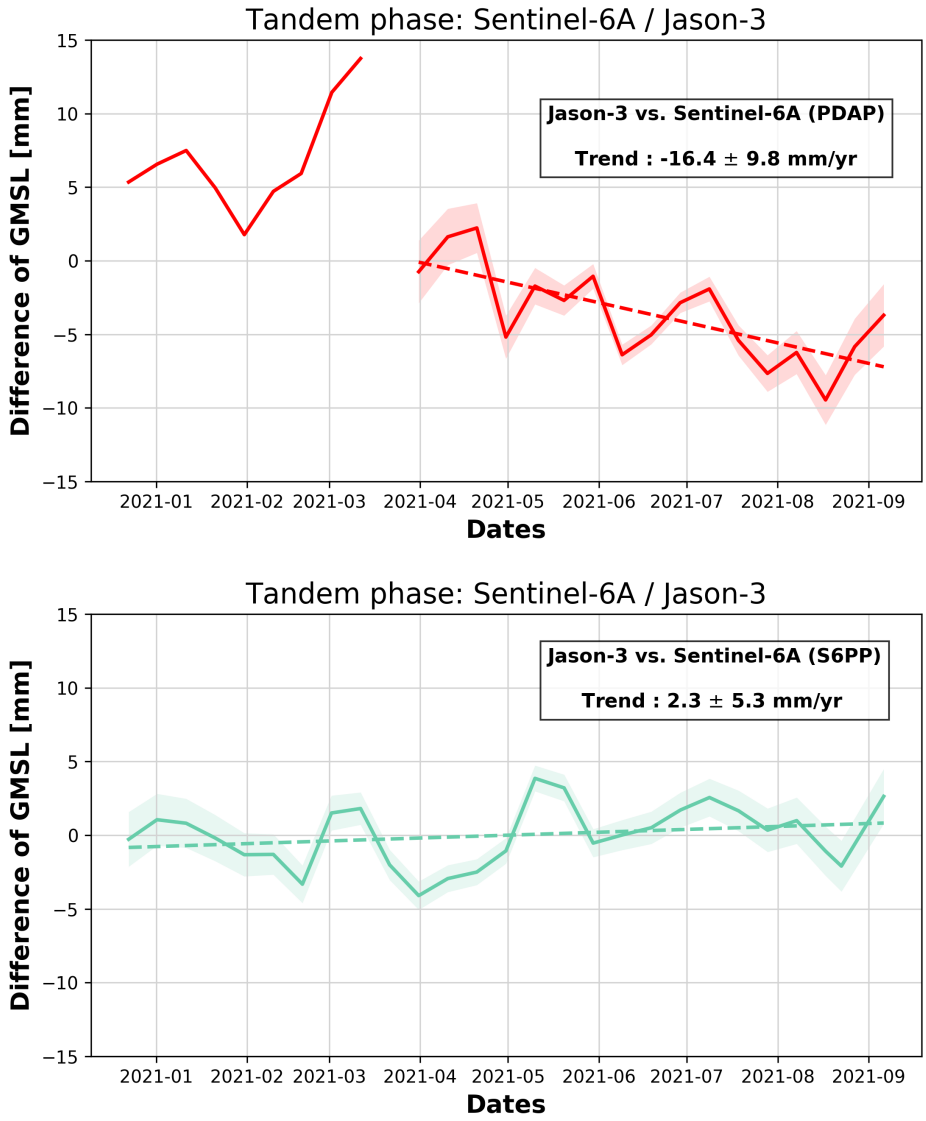

Figure 16: GMSL differences between Jason-3 (GDR-F) and Sentinel-6A MF PDAP data (top), and S6PP data (bottom). The uncertainties are given at the 90% confidence level.

2.2.4.3. Sentinel-6A MF intermission offset with J3

To ensure the long-term stability of the GMSL record with multiple altimetry missions, the intermission GMSL offset calibration is a key element. Following the method develop in Guérou et al. (2022, in prep.), we estimated the intermission offset uncertainty between J3 and S6A, for both PDAP and S6PP data. The method is similar to the one presented in the 2020 annual report (RD3 - Section 2.4.2.1) with a better evaluation of the independent measurements. Since PDAP data is drifting (see Section 2.2.4.2.), estimating an offset between J3 and S6A is highly time sensitive. We expect to observe strong variations of the intermissions offset values with high uncertainties.

In Figure 17, we show the intermissions offset values as a function of the number of cycle used to derive it, with its associated uncertainties, for each S6A datasets. We observe that the PDAP offset is not stable and that the associated uncertainties are large: about 1.6 mm (1-σ) when considering the full tandem phase. Whereas S6PP offset with respect to J3 is rather stable, within 1 mm range, and its uncertainties are way smaller: 0.3 mm (1-σ) when considering the full tandem phase. This latter value is of the order of magnitude of the Jason's series intermissions offset uncertainties (RD3 - Section 2.4.2.1).

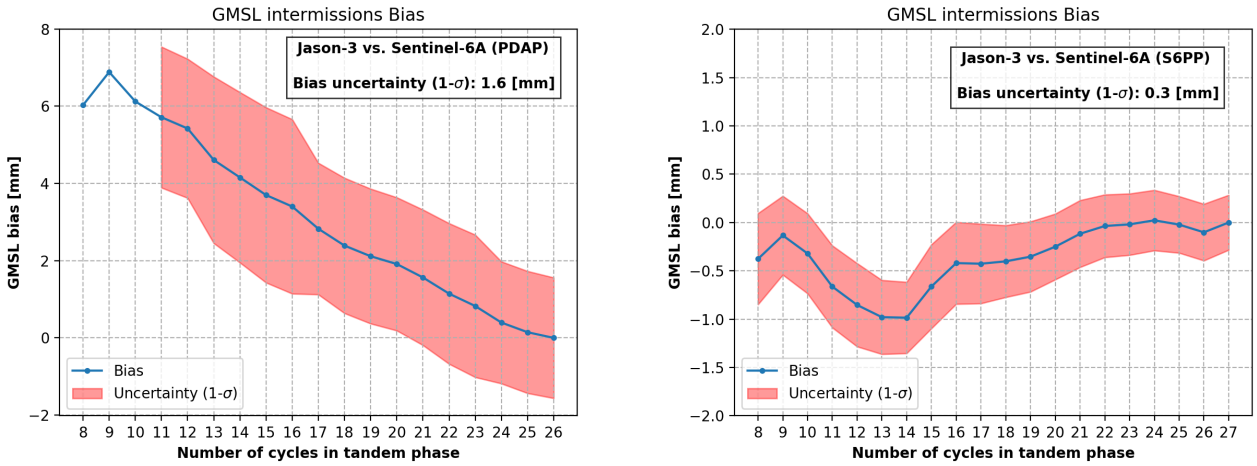

Figure 17: Intermission offset estimations and its associated uncertainties between J3 and S6A PDAP data (left panel) and S6PP data (right panel).

2.2.5. Topex-Poseïdon

In the framework of the TopEx-POSEIDON reprocessing to the standards GDR-F, new investigations on the determination of the offset between TopEx-A and TopEx-B have been performed. The preliminary results are shown in the next Section 2.2.5.1., whereas the comprehensive investigations on the quality of the GDR-F TopEx-POSEIDON GMSL should be published in a peer-review paper in 2022.

2.2.5.1. Intermission offset between TP-A and TP-B

Historically, the offset determination between TopEx-A and TopEx-B has been obtained assuming that the resulting GMSL trend over the period covered by TopEx-POSEIDON (1992-2002) is the most linear possible (CAVE MSL 2009 - see this slide - intern to CLS). The official GDR products of TopEx-POSEIDON are currently based on this processing. The uncertainty associated to this intermission offset estimation has been quantified to $2\ mm$ at 1-σ [17, 16] but no well defined justification currently exists.

The detection of the GMSL acceleration over the altimetry era is offset associated to the study of the Topex instrumental drift (Valladeau et al. [7], Watson et al. [8], Dieng et al. [9], Beckley et al. [10], Cazenave et al. [11], Legeais et al. [12]). But rarely the offset determination between TopEx-A and TopEx-B is mentioned in the litterature as key to this acceleration determination (Kleinherenbrink et al. [18]). However, as mentioned above, a strong assumption has been made on the GMSL trend that dramatically constrains the GMSL acceleration (i. e. , none) over the first ten years of the data record. Kleinherenbrink et al. [18] investigated the topic and found reduced GMSL acceleration when using an other method to estimate the TopEx-A and TopEx-B GMSL offset (crossover difference with ERS mission).

In 2021, we started to revisit the topic and we here present some investigations to better quantify the uncertainty associated to the intermission offset estimation between TopEx-A and TopEx-B when assuming that the GMSL should be the most linear possible over 10-years period.

We used the three other tandem phases between TP/J 1, J 1/J 2 and J 2/J 3 to compare the intermission offsets obtained from the method mentioned above and the one based on the tandem phase data (i. e. „ considered as optimal, see 2020 annual report and Guérou et al., 2022, in prep.). We thus used the full L2P 21 GMSL record that is calibrated from the intermission offset and applied different offsets ranging between $\pm 1\ cm$ at the date of the mission's switch, for each tandem phase, one at a time. We then fit a linear regression over a 10-years period centered on the tandem phase (as done for TopEx-A and TopEx-B) for each offset value and estimate the one that minimize the RMS value of the resulting trend.

Figure 18 shows the GMSL trend RMS values for each switch of missions, for all offset values tested. The zero value offset corresponds to the offset estimates used in the L2P 21 GMSL product. For TopEx-A and TopEx-B (left panel), we naturally found an offset value of zero, as the offset used in the L2P 21 is obtained from the same method (most linear GMSL trend over 10-years). However, for TP/J 1 and J 1/J 2, we find offset values that differ by $1\ mm$ with the values obtained using the tandem phase data. This difference goes up to $2.6\ mm$ for J 2/J 3. This is not surprising since the 10-year period centered around the switch between the two latter missions contains strong ENSO events (in 2010/2011, 2010/2012, 2015/2016 and 2020/2021) that translate into non-linear behavior of the GMSL record. The solution based onto the linear hypothesis is thus strongly affected. Such ENSO events also occurred during TopEx-A and TopEx-B periods (1991/1992, 1994/1995, 1995/1996, 1997/1998 and 1998/1999) that legitimately question the validity of the linear hypothesis. The quality of the offset estimates between TopEx-A and TopEx-B could thus be impacted by the same order of magnitude of discrepancies as for J 2/J 3.

We thus think that the intermission offset uncertainty between TopEx-A and TopEx-B could be revised to higher values, i. e. , $3\ mm$ at $1-\sigma$. Nevertheless, we think that complementary analysis using other altimetry missions should be used to estimate the intermission offset between TopEx-A and TopEx-B (and maybe simultaneously with TopEx-A drift estimation).

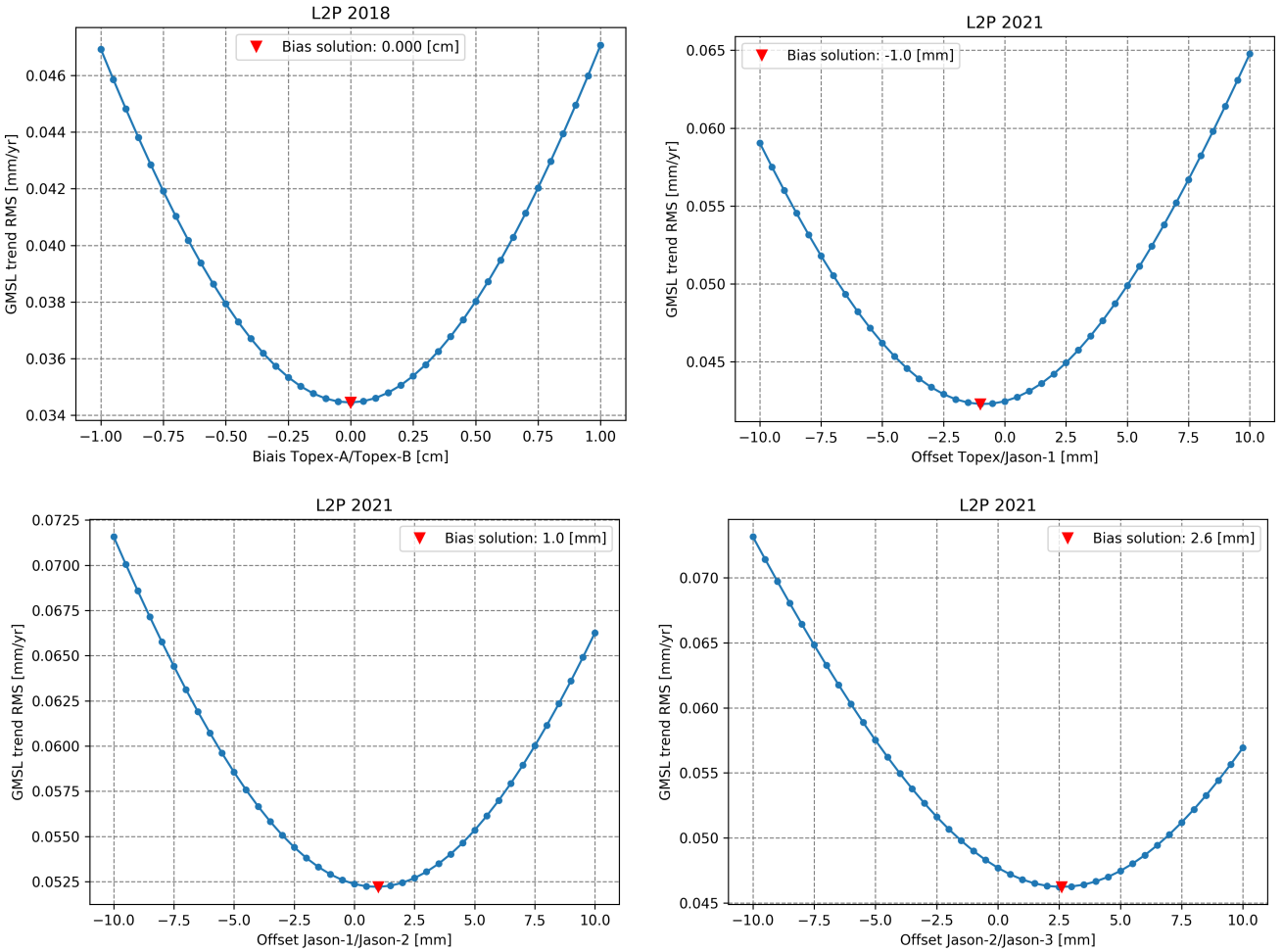

Figure 18: Estimation of the intermission offsets between all the altimetry reference missions: TopEx-A/TopEx-B, TP/J1, J1/J2 and J2/J3. We estimate the offset that minimize the GMSL trend RMS over 10-years period centered around the mision's switches. The imtermission offset values are given relatively to the values used in the L2P21 GMSL.

3. Mean Sea Level from tide-gauges network and comparison with altimetry

In-situ data from Tide-Gauges (TG) networks represent independent sources of sea level measurements that one can use to compare with altimetry. Despite the limited performances of the comparison at the global scale, and even more degraded at the regional scale [2], TG data helps to identify and characterise potential long-term drift and/or discontinuity, i.e. jump, in the altimetry based sea level time series. This has been the case for the first altimetry mission TopEx-POSEIDON [7, 8, 5]

This chapter aims to review the TG networks used at CLS, their data quality, and to give an update of the comparison between altimetry and TG sea level measurements relatively to long-term drift and discontinuity.

3.1. Review of the Tide-Gauges database

In 2020, the TG database has been taken back to operation with the use of the GC and PSMSL networks (see Section 3.1 of RD3). No changes have occurred in 2021.

As a reminder, GC network contains TG "selected for their as-far as possible homogeneous coastline coverage" Ablain et al. [2], and PSMSL is the historical database of TG data. Table 2 summarizes the main characteristics of the these two networks.

Network name	Number of TG	Time Sampling	Area covered	In use
GC	290	Hourly	Global	Yes
PSMSL	1548	Monthly	Global	Yes
REFMAR	87	Sub-hourly	French areas	No
CMEMS	389	Sub-hourly	Europe	No
CNES	6	Sub-hourly	Corsica	No

Table 2: Main characteristics of the Tide-Gauges networks of the CLS database

3.1.1. Data acquisition and processing updates

The data acquisition and processing is described in the 2020 annual report RD3, Section 3.1.1. One change has been made in 2021 for the PSMSL network:

- The atmospheric correction contains the inverse barometer from the ECMWF operational model between 2016-present, and the inverse barometer from the ERA-INTERIM model between 1992-2016.

This modifications has been motivated by the experts on atmospheric correction at CLS and also to follow the choice made for the L2P 21 products. Unfortunately, the inter-calibration between the two atmospheric models has not been considered to estimate the inverse barometer corrections. A jump in the SLA data is thus observed for some TG of the PSMSL data (see Figure 19). Investigations are currently made to correct this anomaly.

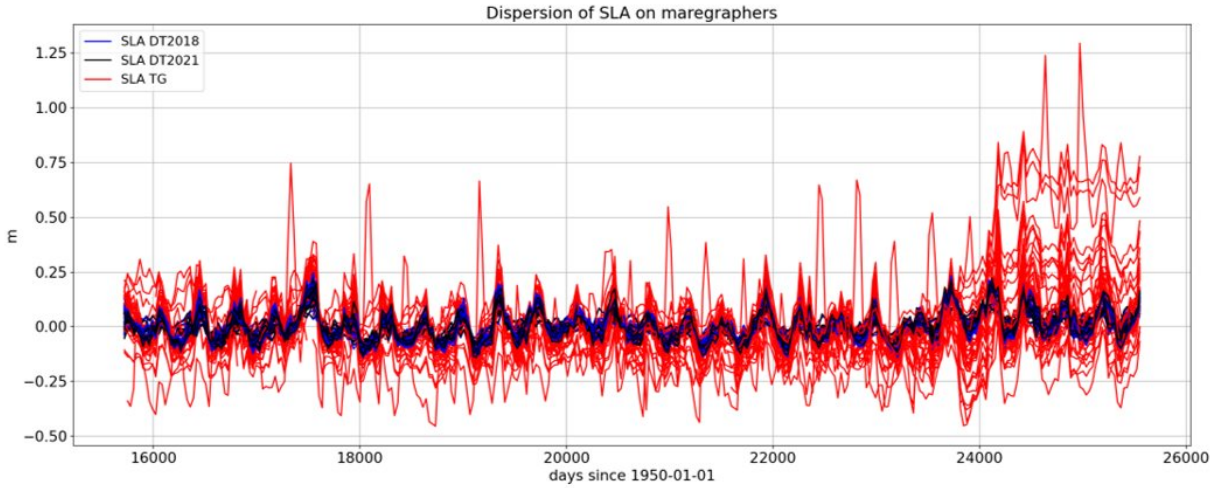

Figure 19: SLA from the PSMSL network TG compared to the SLA from DUACS DT 2018 and DT 2021. A larger dispersion and some jumps are observed from the Julian day 24100, i. e. , corresponding to February 2016.

The last data acquisition on the CLS database has been performed on **the 12th of December 2021**. It thus contains all data of GC and PSMSL networks that were available at that time (see Figure 20).

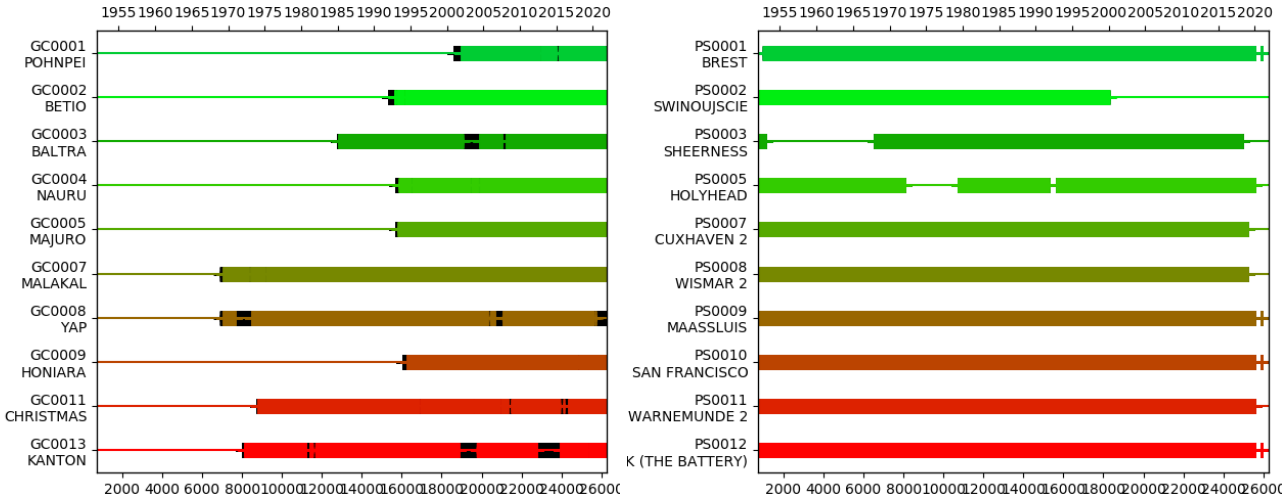

Figure 20: Example of the database status control for the GC (left) and PSMSL network (right). Such quality controls are subject to evolve (see Section 3.1.2 of the 2020 annual report)

3.1.2. Status of the AVISO webpages

The Tide-Gauges data from the CLS database are not directly distributed onto the AVISO website. However, the comparison of TG data to the altimetry sea level measurements are distributed through synthetic sheets (not updated since November 2016 on the website). However, internal updates are now regularly performed for the GC and PSMSL network since 2021. On-demand request can be sent by email to CLS to get access to these results.

Examples of the updated version are given in Figure 21 for GC 0001, and in Figure 22 for PS 0001.

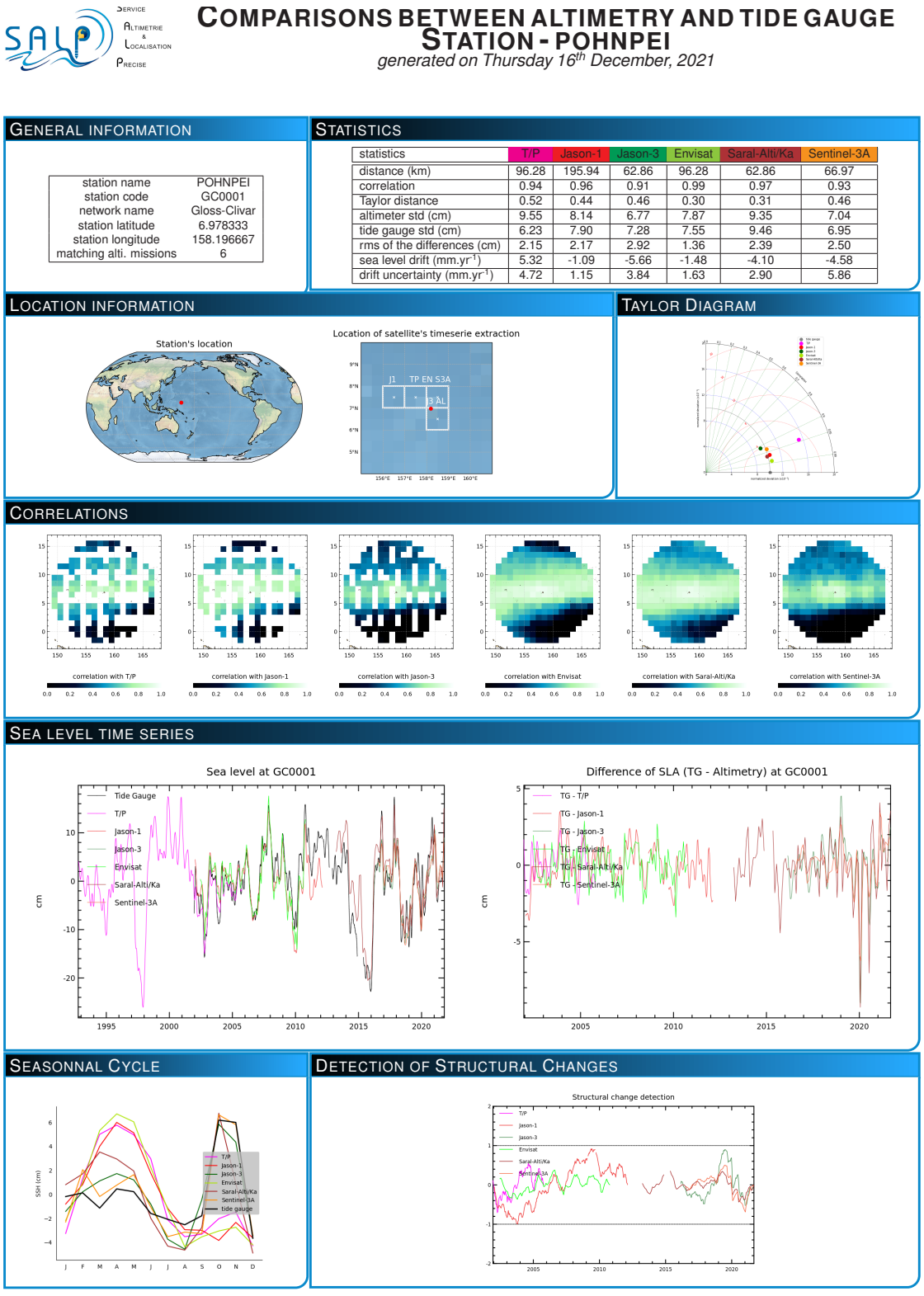

Figure 21: Example of Tide-Gauges comparison between GC0001 and all altimetry missions. This version has been updated in 2021 but is still not distributed on AVISO.

SERVICE ALTIMETRIE & LOCALISATION PRECISE

COMPARISONS BETWEEN ALTIMETRY AND TIDE GAUGE STATION - BREST

generated on Thursday 16th December, 2021

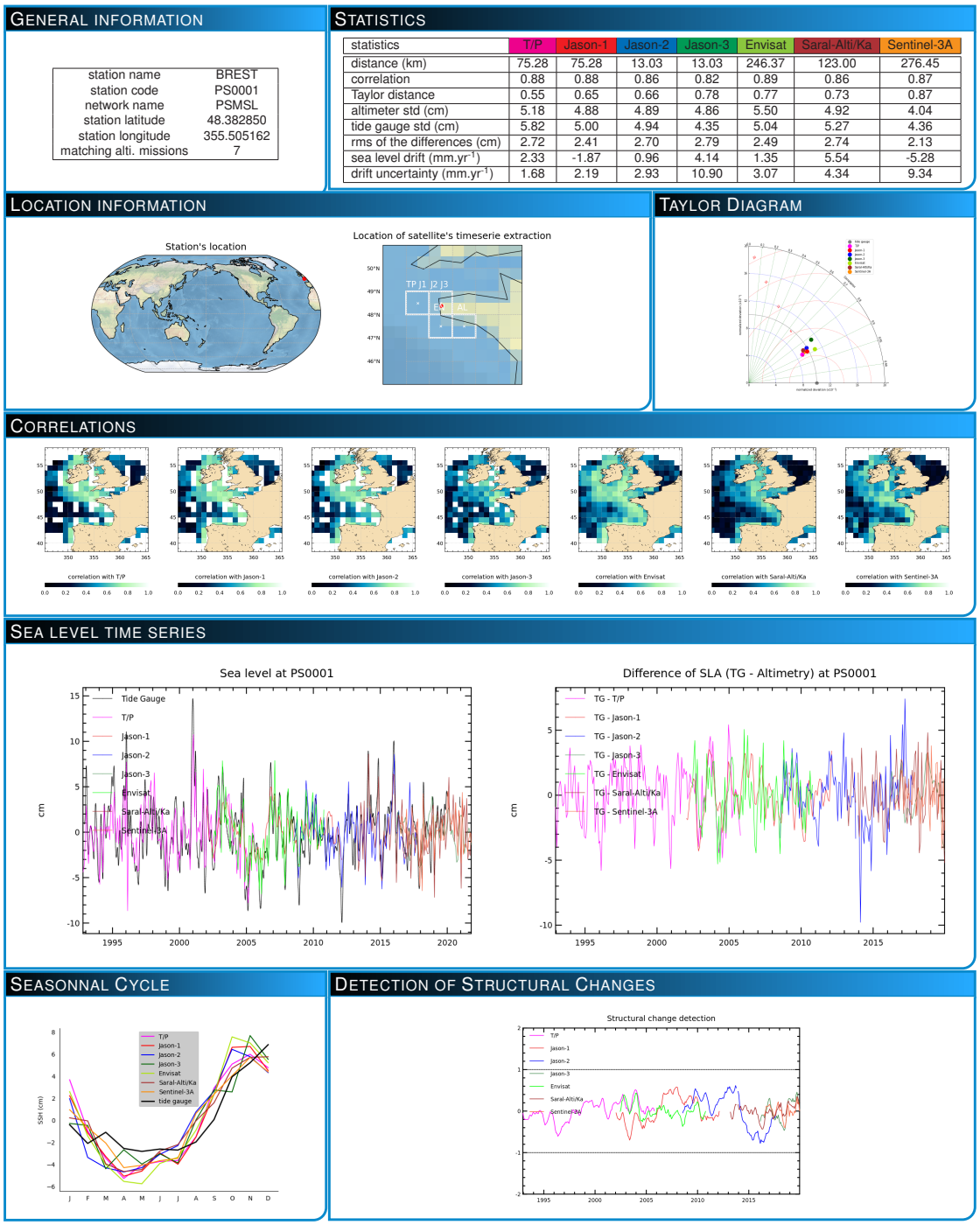

station name	BREST
station code	PS0001
network name	PSMSL
station latitude	48.382850
station longitude	355.505162
matching alti. missions	7

statistics	T/P	Jason-1	Jason-2	Jason-3	Envisat	Saral-Alti/Ka	Sentinel-3A
distance (km)	75.28	75.28	13.03	13.03	246.37	123.00	276.45
correlation	0.88	0.88	0.86	0.82	0.89	0.86	0.87
Taylor distance	0.55	0.65	0.66	0.78	0.77	0.73	0.87
altimeter std (cm)	5.18	4.88	4.89	4.86	5.50	4.92	4.04
tide gauge std (cm)	5.82	5.00	4.94	4.35	5.04	5.27	4.36
rms of the differences (cm)	2.72	2.41	2.70	2.79	2.49	2.74	2.13
sea level drift (mm.yr^{-1})	2.33	-1.87	0.96	4.14	1.35	5.54	-5.28
drift uncertainty (mm.yr^{-1})	1.68	2.19	2.93	10.90	3.07	4.34	9.34

Figure 22: Example of Tide-Gauges comparison between PS 0001 and all altimetry missions. This version has been updated in 2021 but is still not distributed on AVISO.

3.2. Comparison of GMSL from Tide-Gauges and altimetry missions

In this section, we compare Tide-Gauges data from the database described in Section 3.1. with sea levels records from altimetry missions. Such comparison allows to detect drifts and/or discontinuity in either the altimeter or the in-situ records. We follow the method described in Prandi et al. [1], Ablain et al. [2] and summarised in RD3 (Section 3.3.2) that uses an error budget to estimate drift uncertainties. Details of this error budget is given in section 3.2.1.. The results of the comparisons between TG data and altimetry missions are given in Section 3.2.2. for the in-flight missions and in Section 3.2.3. for the reference missions.

3.2.1. Error budget estimation

The construction of the altimetry-TG error budget, as described in Ablain et al. [2], contains the following sources of errors:

- **Annual and sub-annual correlated errors**. The exact origins of these errors are unknown and directly measured on the altimetry-TG time series. We suspect TG and altimeter measurement errors and/or collocation errors of both datasets to significantly contribute to these errors. They are therefore dependent on the altimetry mission considered as well as the in-situ network used. The associated uncertainties are measured as the standard deviation of the altimetry-TG difference noise at the respective timescales (6-months and 1-year).
- **Inter-annual to decadal correlated errors**. The exact origins of these errors are unknown but they principally affect the TG data (i. e. , TG networks averaging method, long-term stability of TG time series, etc.). The uncertainties have been estimated in Ablain, Taburet, Zawadzki, Jugier, and Vayre [2] (see also Ablain et al., 2018, from the 25 years of altimetry conference) by taking the standard deviation of the altimetry-TG drift distribution for periods lengths of 3 years and 10 years, divided by the square root of the independent tide-gauge number.
- **Drifts uncertainties**, that corresponds to the VLM that are not corrected for in the TG data post-processings. These uncertainties only depends on the in-situ networks and are non-correlated between each tide gauge. The global trend uncertainty is $\sigma / \sqrt{N}$ where σ is the average VLM uncertainty for each TG and N is the number of TG.
- **Intermissions offset uncertainties**, that correspond to the uncertainties to connect two successive altimetry missions over time. These uncertainties apply only to the reference missions TP, J 1, J 2 and J 3. The bias errors made when connecting TG time series are not considered here. First, these errors are difficult to quantify. Second, we assumes that these errors are taken into account into the high-frequency noise that one measure on the respective time series. This is of course an approximation and a limitation to the method.

As one can understand from the short description above, the uncertainty budget depends on the altimetry missions (and the geophysical standards used), on the in-situ network, and implicitly on the length of the time series. In 2021, we were able to update the uncertainty budget values for all the in-flight missions as well as for reference missions. Table 3 gives the uncertainty budget we used here for each missions for both the GC and PSMSL networks. We used the value mentioned in [2, section 3.3.3.2, Table 7] for the VLM uncertainty estimations and measured the uncertainties associated to the correlated errors directly on the respective timeseries from a filtering method (as for the GMSL uncertainty budget presented in Section 2.2.1..

Temporal correlation	Network	Uncertainty at 1-σ [mm]						
		TP	J1	J2	J3	Saral	S3A(SAR/PLRM)	S3B(SAR/PLRM)
$\lambda = 6$ months	GC	3.9	3.3	4.2	3.2	1.5	1.3 / 1.4	1.8 / 1.8
	PSMSL	2.7	2.4	3.0	2.8		2.9 / 2.9	
$\lambda = 1$ year	GC	1.1	0.6	1.3	0.5	0.4	0.5 / 0.4	1.3 / 0.4
	PSMSL	1.2	1.1	1.3	0.9		1.1 / 1.0	
$\lambda = 3$ years	GC/PSMSL	1						
$\lambda = 10$ years	GC/PSMSL	1						
Drift error	GC/PSMSL	0.2						

Table 3: Error budget for the estimation of GMSL drifts between altimetry and Tide-Gauges networks (GC and PSMSL). The VLM value come from the estimation made in 2018 [2] as well as for the correlated errors at 3- and 10-years timescales, see the text for more details.

3.2.2. Drift analyses of the missions in-flight

We here show and analyse the GMSL comparisons between the TG data from both GC and PSMSL network and the various altimetry missions in-flight: Jason-3, Saral/AltiKa, Sentinel-3A and Sentinel-3B. We used the GDR-F data for both J3 and Saral, and the last PDGS reprocessing data for S3A and S3B.

- **Jason-3**
  On Figure 23, a drift of $0.5 \pm 1.5\, mm/yr$ at 90% CL is observed as when using the GC network (blue curve) and $0.7 \pm 2.2\, mm/yr$ with PSMSL network (red curve). These drifts are not significant even though the trend are quite homogeneous over the first five years of data. The uncertainties are quite large and do not allow to analyse the potential drift of the radiometer (see Section 2.2.1.1..

- **Saral/AltiKa**
  No drift is detected for this mission ($-0.4 \pm 0.7\, mm/yr$, see Figure 24) when compared to the GC network. The long period studied explains the low uncertainty obtained. It is important to notice that the change of orbit that occurred in mid-2016 is not taken into account into the error budget. Still, no clear changes are observed at this time. However, we observe that the signal tend to start drifting from 2019-present, non- significantly, but it is interesting to notice as we observe similar behavior of Saral/AltiKa mission when comparing to Jason-3 GMSL (see Figures 3 and Figure 11). Such drift could potentially come from the systematic miss-pointing observed since 2019 (see also the Saral 2021 annual report).

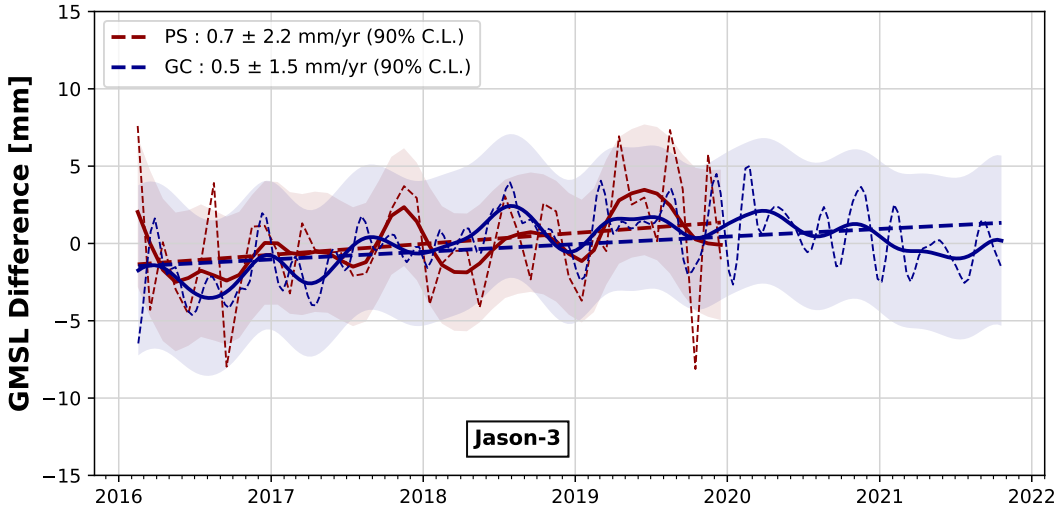

Figure 23: Drift estimation between GC network and the J3 mission

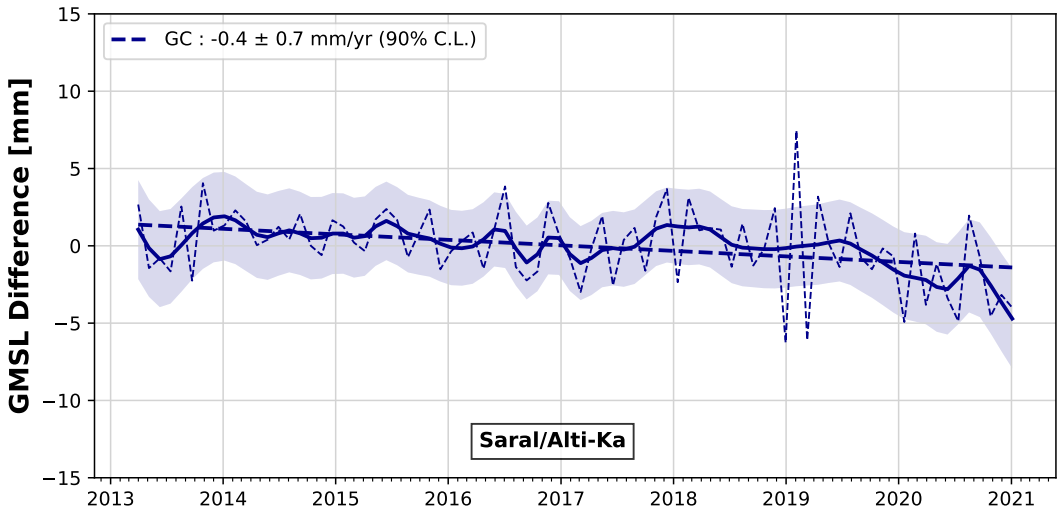

Figure 24: Drift estimation between GC network and the Saral mission

- **Sentinel-3A**
  This mission is known to be impacted by a large drift of its SAR mode Ablain et al. [19, see also Section 2.2.2.] of about $1.3\,mm/yr$ whereas its PLRM mode shows smaller drift of about $0.3\,mm/yr$. Such drifts are barely detectable with the in-situ comparison method presented here given the large uncertainties : we find drifts of $1.4 \pm 2.5\,mm/yr$ and $0.7 \pm 0.9\,mm/yr$ for the SAR mode as compared to PSMSL and GC, respectively. And $0.8 \pm 2.5\,mm/yr$ and $0.3 \pm 0.9\,mm/yr$ for the PLRM mode. We note that the uncertainties associated to the PSMSL comparison are larger and this is mainly due to the shorter period available for comparison.

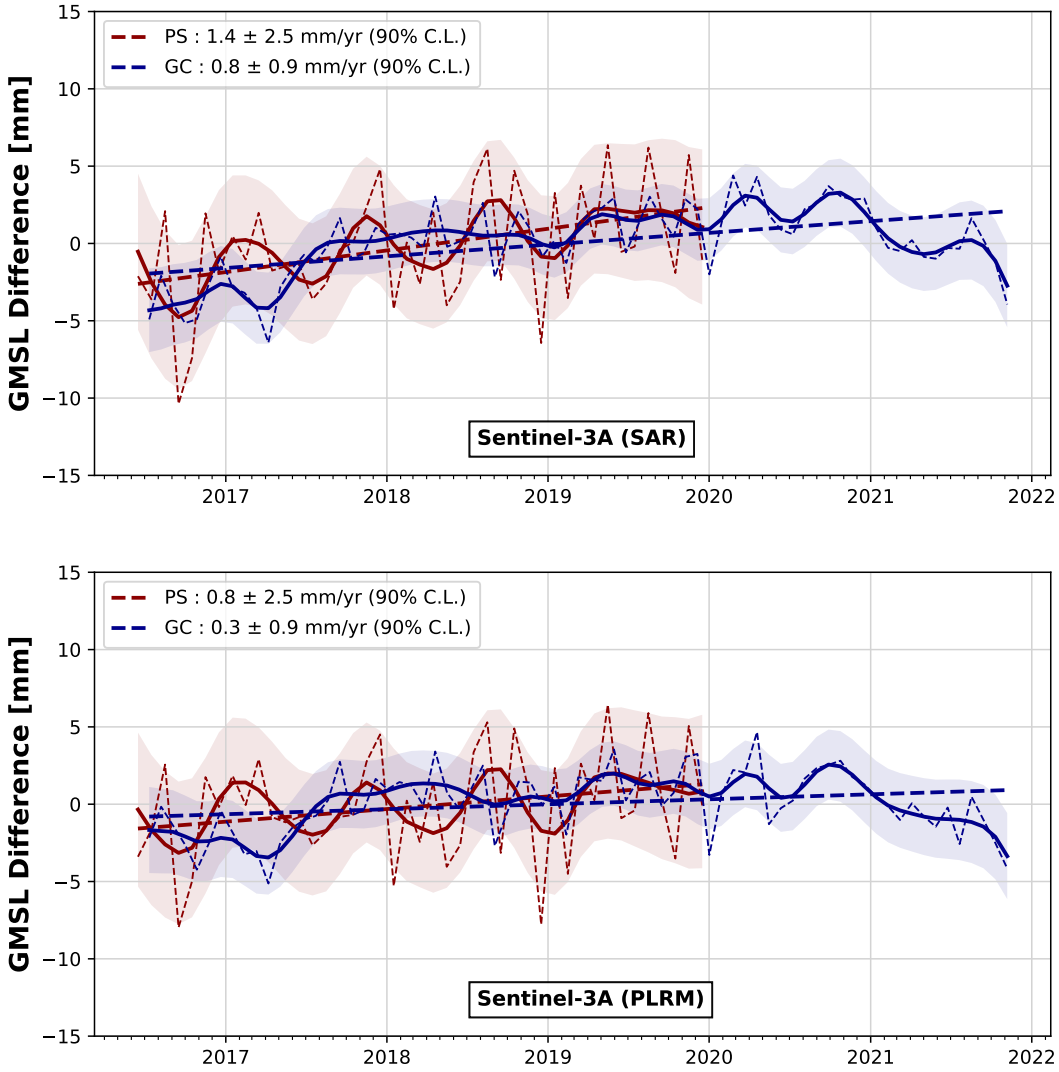

Figure 25: Drift estimation between GC network and the S3A mission, in SAR mode (top) and PLRM mode (bottom)

- **Sentinel-3B**
  As presented in Section 2.2.3., this mission is affected by a long-term drift of $\sim 3 mm.yr^{-1}$ due to an anomaly in the ground processing. Despite the short time period available, such drift starts to be detectable with the TG comparison. Indeed, in Figure 26, we show that we detect drifts of $-3.8 \pm 2\, mm/yr$ for the SAR mode, and $-3.0 \pm 1.7\, mm/yr$ for the PLRM mode as compare to the GC network. The values found have the correct sign (negative, i. e. , trend underestimated) and the same order of magnitude ($\sim 3 mm.yr^{-1}$) than the expected anomaly. This example shows the interest of the in-situ comparison with TG to detect strong long-term drifts.

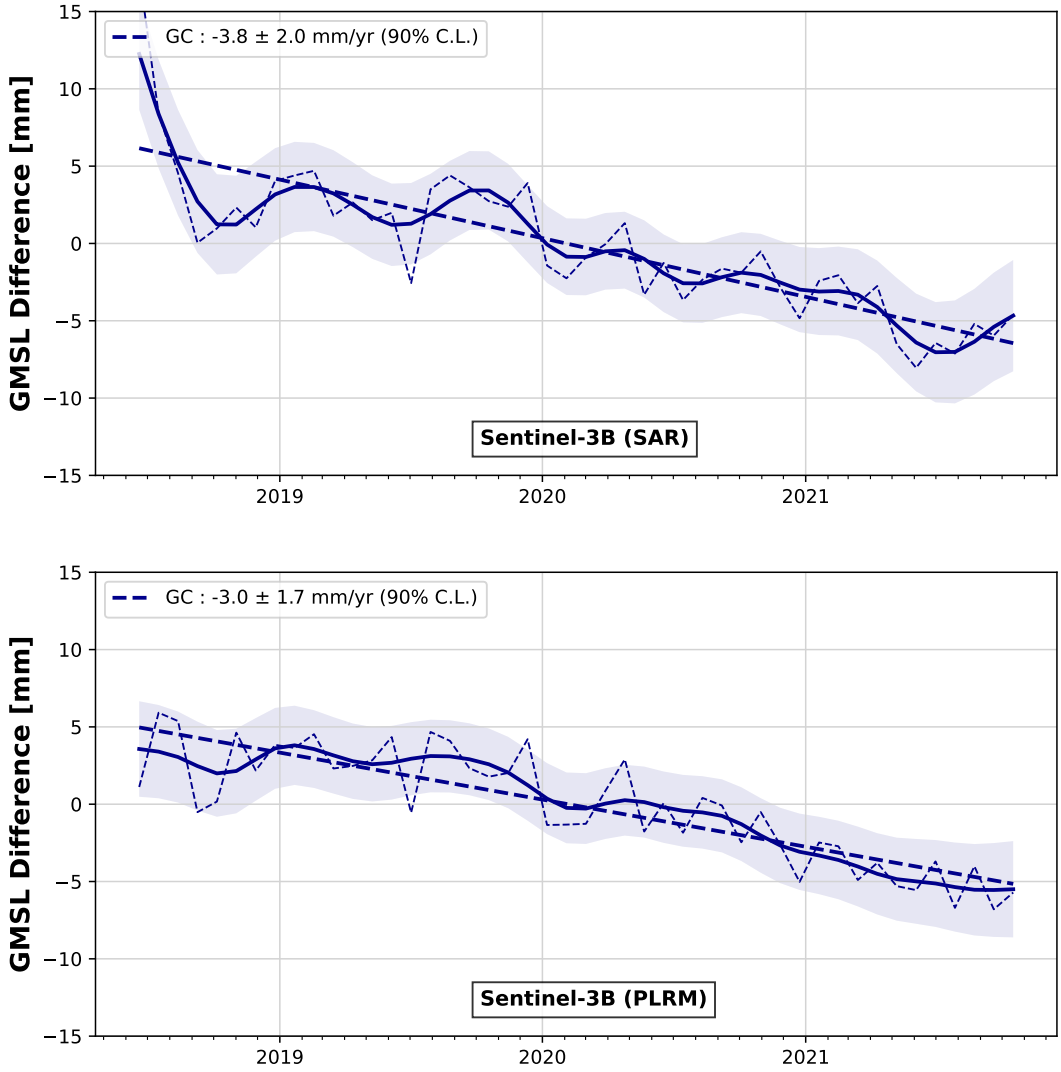

Figure 26: Drift estimation between GC network and the S3A mission, in SAR mode (top) and PLRM mode (bottom)

3.2.3. Drift analyses of the reference missions

In Figure 27, we show the difference between the GMSL obtained from the reference missions (TP, J 1, J 2, and J 3) and the GC and PSMSL TG data. As compare to the 2020 annual report [RD3], we use the L2P 21 GMSL data and therefore add two years of data to compare wiwth the GC network. We also show this year the comparison to PSMSL network. Some issues with the PSMSL network data remains and are easily is observed between 2014-2016. The exact origin is under investigation but non-homogeneous updates in the atmospheric correction used for this network is suspected (see Section 3.1.1.).

We observed null drifts with respect to GC and PSMSL networks with rather small uncertainties of $0.5\ mm.yr^{-1}$. The larger variations (and drift) during the TopEx-POSEIDON period is still visible, as expected (L2P 21 standards do not include reprocessed data of TP as compare to the L2P 18 standards)

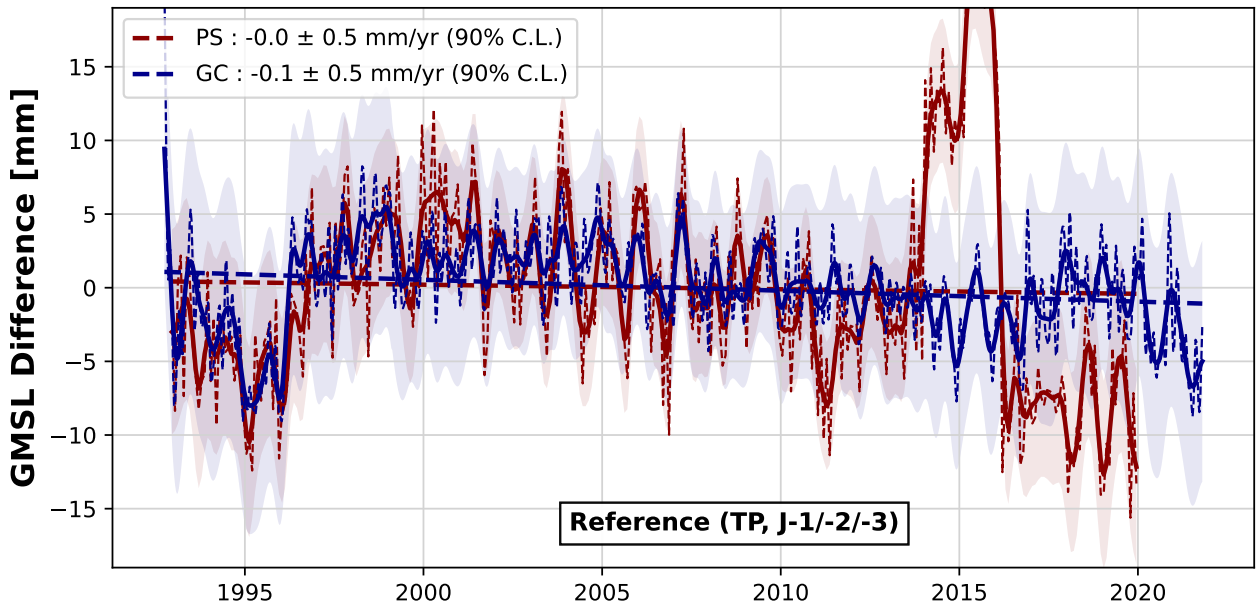

Figure 27: Drift estimation between GC network and the reference missions

References

[1] P. Prandi, G. Valladeau, and V. Debout, "Validation of altimeter data by comparison with tide gauges measurements: yearly report 2016," *SALP - Yearly report*, no. 1 rev 1, 2016. [Online]. Available: https://www.aviso.altimetry.fr/fileadmin/documents/calval/validation_report/annual_report_TG_2016.pdf

[2] M. Ablain, N. Taburet, L. Zawadzki, R. Jugier, and M. Vayre, "SALP annual report (2017) of Mean Sea Level Activities," no. 2017, 2018. [Online]. Available: https://www.aviso.altimetry.fr/fileadmin/documents/calval/validation_report/SALP-RP-MA-EA-23189-CLS_AnnualReport_2017_MSL.pdf

[3] A. Guérou, "SALP annual report on Mean Sea Level from Altimetry and Tide-Gauges," Tech. Rep., 2020.

[4] H. Roinard and J. Coquelin, "CalVal Jason-3 validation of GDR-F data over ocean," Tech. Rep., 2021. [Online]. Available: https://www.aviso.altimetry.fr/fileadmin/documents/calval/validation_report/J3/SALP-RP-MA-EA-23480-CLS_Jason3_Reprocessing_Report_v1-2.pdf

[5] M. Ablain, R. Jugier, L. Zawadzki, N. Taburet, A. Cazenave, B. Meyssignac, and N. Picot, "The TOPEX-A drift and impacts on GMSL time series Comparison with Poseïdon," p. 2017, 2017. [Online]. Available: https://meetings.aviso.altimetry.fr/fileadmin/user_upload/tx_ausyclsseminar/files/Poster_OSTST17_GMSL_Drift_TOPEX-A.pdf

[6] A. Barnoud, J. Pfeffer, A. Guérou, M. Frery, M. Siméon, A. Cazenave, J. Chen, W. Llovel, V. Thierry, J. Legeais, and M. Ablain, "Contributions of Altimetry and Argo to Non-Closure of the Global Mean Sea Level Budget Since 2016," *Geophysical Research Letters*, vol. 48, no. 14, jul 2021.

[7] G. Valladeau, J. F. Legeais, M. Ablain, S. Guinehut, and N. Picot, "Comparing Altimetry with Tide Gauges and Argo Profiling Floats for Data Quality Assessment and Mean Sea Level Studies," *Marine Geodesy*, vol. 35, no. sup1, pp. 42–60, dec 2012. [Online]. Available: https://www.tandfonline.com/doi/full/10.1080/01490419.2012.718226

[8] C. S. Watson, N. J. White, J. A. Church, M. A. King, R. J. Burgette, and B. Legresy, "Unabated global mean sea-level rise over the satellite altimeter era," *Nature Climate Change*, vol. 5, no. 6, pp. 565–568, jun 2015. [Online]. Available: http://www.nature.com/articles/nclimate2635

[9] H. B. Dieng, A. Cazenave, B. Meyssignac, and M. Ablain, "New estimate of the current rate of sea level rise from a sea level budget approach," *Geophysical Research Letters*, vol. 44, no. 8, pp. 3744–3751, apr 2017. [Online]. Available: http://doi.wiley.com/10.1002/2017GL073308

[10] B. D. Beckley, P. S. Callahan, D. W. Hancock, G. T. Mitchum, and R. D. Ray, "On the "Cal-Mode" Correction to TOPEX Satellite Altimetry and Its Effect on the Global Mean Sea Level Time Series," *Journal of Geophysical Research: Oceans*, vol. 122, no. 11, pp. 8371–8384, nov 2017. [Online]. Available: http://doi.wiley.com/10.1002/2017JC013090

[11] A. Cazenave, B. Meyssignac, M. Ablain, M. Balmaseda, J. Bamber, V. Barletta, B. Beckley, J. Benveniste, E. Berthier, A. Blazquez, T. Boyer, D. Caceres, D. Chambers, N. Champollion, B. Chao, J. Chen, L. Cheng, J. A. Church, S. Chuter, J. G. Cogley, S. Dangendorf, D. Desbruyères, P. Döll, C. Domingues, U. Falk, J. Famiglietti, L. Fenoglio-Marc, R. Forsberg, G. Galassi, A. Gardner, A. Groh, B. Hamlington, A. Hogg, M. Horwath, V. Humphrey, L. Husson, M. Ishii, A. Jaeggi, S. Jevrejeva, G. Johnson, N. Kolodziejczyk, J. Kusche, K. Lambeck, F. Landerer, P. Leclercq, B. Legresy, E. Leuliette, W. Llovel, L. Longuevergne, B. D. Loomis, S. B. Luthcke, M. Marcos, B. Marzeion, C. Merchant, M. Merrifield, G. Milne, G. Mitchum, Y. Mohajerani, M. Monier, D. Monselesan, S. Nerem,

H. Palanisamy, F. Paul, B. Perez, C. G. Piecuch, R. M. Ponte, S. G. Purkey, J. T. Reager, R. Rietbroek, E. Rignot, R. Riva, D. H. Roemmich, L. S. Sørensen, I. Sasgen, E. J. Schrama, S. I. Seneviratne, C. K. Shum, G. Spada, D. Stammer, R. van de Wal, I. Velicogna, K. von Schuckmann, Y. Wada, Y. Wang, C. Watson, D. Wiese, S. Wijffels, R. Westaway, G. Woppelmann, and B. Wouters, "Global sea-level budget 1993–present," *Earth System Science Data*, vol. 10, no. 3, pp. 1551–1590, aug 2018. [Online]. Available: https://essd.copernicus.org/articles/10/1551/2018/

[12] J. Legeais, W. Llovel, A. Melet, and B. Meyssignac, "Evidence of the TOPEX-A Altimeter Instrumental Anomaly and Acceleration of the Global Mean Sea Level," *Copernicus Marine Service Ocean State Report - Journal of Operational Oceanography*, vol. 13, no. 4, pp. Issue Sup 1, s77, 2020.

[13] G. Taburet, A. Sanchez-Roman, M. Ballarotta, M.-I. Pujol, J.-F. Legeais, F. Fournier, Y. Faugere, and G. Dibarboure, "DUACS DT2018: 25 years of reprocessed sea level altimetry products," *Ocean Science*, vol. 15, no. 5, pp. 1207–1224, sep 2019. [Online]. Available: https://os.copernicus.org/articles/15/1207/2019/

[14] D. Stammer, A. Cazenave, R. M. Ponte, and M. E. Tamisiea, "Causes for Contemporary Regional Sea Level Changes," *Annual Review of Marine Science*, vol. 5, no. 1, pp. 21–46, jan 2013. [Online]. Available: http://www.annualreviews.org/doi/10.1146/annurev-marine-121211-172406

[15] R. Jugier, M. Ablain, R. Fraudeau, A. Guerou, and P. Féménias, "On the uncertainty associated with detecting global and local mean 1 sea level drifts on Sentinel-3A and Sentinel-3B altimetry missions," *Ocean Science Discussions*, vol. 2021, pp. 1–23, 2021. [Online]. Available: https://doi.org/10.5194/os-2021-106

[16] M. Ablain, B. Meyssignac, L. Zawadzki, R. Jugier, A. Ribes, G. Spada, J. Benveniste, A. Cazenave, and N. Picot, "Uncertainty in satellite estimates of global mean sea-level changes, trend and acceleration," *Earth System Science Data*, vol. 11, no. 3, pp. 1189–1202, aug 2019. [Online]. Available: https://www.earth-syst-sci-data-discuss.net/essd-2019-10/https://essd.copernicus.org/articles/11/1189/2019/

[17] L. Zawadzki and M. Ablain, "Accuracy of the mean sea level continuous record with future altimetric missions: Jason-3 vs. Sentinel-3a," *Ocean Science*, vol. 12, no. 1, pp. 9–18, jan 2016. [Online]. Available: https://www.ocean-sci.net/12/9/2016/https://os.copernicus.org/articles/12/9/2016/

[18] M. Kleinherenbrink, R. Riva, and R. Scharroo, "A revised acceleration rate from the altimetry-derived global mean sea level record," *Scientific Reports*, vol. 9, no. 1, dec 2019.

[19] M. Ablain, R. Jugier, B. Meyssignac, A. Guerou, S. Labroue, M. Raynal, and J. Poisson, "Estimation and impact of Sentinel-3a GMSL drift on climate-driven studies," 2019. [Online]. Available: https://meetings.aviso.altimetry.fr/fileadmin/user_upload/2019/SC1_01_s3a_gmsl_drft_ablain.pdf